古 脊 椎 动 物 学 报
VERTEBRATA PALASIATICA

DOI: 10.19615/j.cnki.2096-9899.260616
CSTR: 32090.14.j.cnki.2096-9899.260616

A new feathered dinosaur from Early Cretaceous of northern China highlighting the complexity of early pennaraptoran evolution and comments on several relevant conceptual and methodological issues

XU Xing

(Institute of Vertebrate Paleontology and Paleoanthropology, Chinese Academy of Sciences, Beijing, 100044)

Abstract Recent discoveries of early-diverging pennaraptoran fossils have shed light on the origin of birds and, in particular, the evolution of defining avian features such as pennaceous feathers and flight capability. Here I report a new pennaraptoran dinosaur based on a fossil recovered from the Lower Cretaceous Jiufotang Formation of western Liaoning, China. Despite exhibiting a combination of derived features observed across distinct pennaraptoran lineages, this new taxon is likely an early-diverging deinonychosaurian. Most notably, it possesses exceptional plumage characteristics: it represents the first known early-diverging pennaraptoran to bear both large pedal feathers and highly elongated rectrices; these elongated rectrices are substantially more abundant than those of other early-diverging pennaraptorans, bearing a superficial resemblance to the tail plumes of peacocks; and its wing feathers form the proportionally largest feathered wings among non-avialan pennaraptorans—even with relatively short bony forelimbs—indicating a decoupling of forelimb skeletal length and feathered wing surface area. This discovery underscores the complexity of early pennaraptoran evolution and raises several conceptual and methodological issues in pennaraptoran research. These issues include how to recover a robust pennaraptoran phylogeny, how to infer the aerial behavior and habitat ecology of early-diverging pennaraptorans, and how to define feathers and birds. I briefly address these issues in this paper.

Key words Jianchang, Liaoning; Early Cretaceous; Jiufotang Formation; Pennaraptora; feathers; phylogeny; morphology; habitat ecology and aerial behavior

1 Introduction

Pennaraptoran dinosaurs represent a group of theropod dinosaurs comprising four long-recognized major clades (i.e., Oviraptorosauria, Dromaeosauridae, Troodontidae and Avialae). Several recently discovered small clades (e.g., Unenlagiinae (Novas and Puerta, 1997; Bonaparte, 1999), Microraptorinae (Xu et al., 1999; Senter et al., 2004; Xu and Wang, 2004), Scansoriopterygidae (Czerkas and Yuan, 2002; Zhang et al., 2002; Zhang et al., 2008; Xu et al., 2015), Anchiornithinae (Xu et al., 2009a; Xu et al., 2016; Foth and Rauhut, 2017), and

国家重点研发计划(编号：2025YFF0811700)和国家自然科学基金基础中心项目(批准号：42288201)资助。

收稿日期：2026-05-08

Halszkaraptorinae (Cau et al., 2017)) are also assigned to Pennaraptora, yet their phylogenetic affinities with these four major pennaraptoran clades remain unresolved. Nevertheless, over the past three decades, spectacular fossils from both the newly recognized minor clades and the long-established major pennaraptoran groups have substantially filled morphological gaps among major pennaraptoran lineages, yielded the earliest known fossil record of feathers, documented the earliest instances of theropod flight, uncovered unexpected morphologies and ecological adaptations, and evidenced a rapid radiation of Pennaraptora during the Middle Jurassic (Zhou and Zhang, 2002; Norell and Xu, 2005; Hu et al., 2009; Brusatte, 2011; Xu et al., 2014a; Brusatte et al., 2015; Foth and Rauhut, 2017; Pittman and Xu, 2020; Chen et al., 2025). Notably, these fossils have substantially advanced our understanding of avian origins, revealing that pennaceous feathers, aerodynamic behaviors, and other hallmarks once considered exclusive to Avialae occur in other pennaraptoran groups (Xu et al., 2014a; Brusatte et al., 2015; Pittman and Xu, 2020). Furthermore, the transition to birds was highly complex (Xu et al., 2015; Agnolín et al., 2019), involving extensive evolutionary experimentation and reversals. However, numerous critical issues remain unresolved, including those related to reconstructing pennaraptoran phylogeny, behavior, and ecology—as well as the interpretation of individual morphological characters (Xu et al., 2014a; Pittman and Xu, 2020). For instance, the discovery of large hindlimb feathers in some early-diverging pennaraptorans represents a key advance in understanding feather evolution and the origin of theropod flight. Nonetheless, ongoing debates persist regarding which taxa possessed such feathers and whether large pennaceous hindlimb feathers served aerodynamic functions in these forms (Padian, 2003; Xu et al., 2003; Chatterjee and Templin, 2007; Alexander et al., 2010; Dyke et al., 2013; Evangelista et al., 2014; Palmer, 2014; Manafzadeh and Padian, 2018). Such controversy stems partly from the fact that avian traits were likely shaped by multiple interacting factors (e.g., inheritance, function, and ecology), and that biological structures frequently served multiple functional roles (e.g., the diverse functions of feathers). Debates also arise because observed fossil morphologies may not represent genuine biological features: for instance, the purported absence of large hindlimb feathers in some taxa is likely a preservational artifact (Xu and Barrett, 2025). This uncertainty impacts not only our understanding of individual species but also robust reconstructions of clade-level evolutionary history.

Here I report a new pennaraptoran dinosaur based on a specimen collected from the Lower Cretaceous Jiufotang Formation of western Liaoning, China (Figs. 1, 2). The specimen preserves a nearly complete skeleton associated with extensive plumage across the entire body. It exhibits a unique combination of derived features observed in distinct pennaraptoran lineages, representing a new four-winged theropod taxon and underscoring the complexity of character evolution during the transition to birds.

In the following text, I describe the three tetanuran manual digits as II-III-IV as in most ornithological and some paleontological literature (Feduccia, 1999; Xu et al., 2009b); for the convenience, I use Oviraptorosauria, Dromaeosauridae, and Troodontidae in a narrow sense (i.e., Scansoriopterygidae, Unenlagiinae, and Anchiornithinae are not respectively included in these clades).

2 Systematic palaeontology

Theropoda Marsh, 1881

Maniraptora Gauthier, 1986

Pennaraptora Foth et al., 2014

***Changzhousaurus sinensis* gen. et sp. nov**

(Figs. 1-14)

LSID: urn:lsid:zoobank.org:pub:DDDBF69B-C9BD-429B-9C71-6CA22924CD0C

Etymology *Changzhou*, Latin for Changzhou (a city in Jiangsu Province, China); *saurus,* Latinization of Greek for lizard. The genus name is to thank Changzhou Municipal Government for supporting dinosaur palaeontology and promoting popular science. The specific epithet is to highlight the birthplace of this amazing dinosaur (China).

Holotype LDNHMF 2026A and 2026B (housed at the Lande Museum of Natural History, Tangshan, Hebei Province, China), a nearly complete skeleton with associated plumage preserved on a slab (2026A) and a counter slab (2026B). Casts of both slab and counter slab of this specimen are housed at the Institute of Vertebrate Paleontology and Paleoanthropology, Chinese Academy of Sciences (catalogued as IVPP FV2204A and 2204B).

Type locality and horizon Lamadong, Jianchang, western Liaoning Province; Lower Cretaceous (Aptian) Jiufotang Formation (Yu et al., 2021).

Diagnosis A small pennaraptoran theropod with the following autopomorphies: a premaxilla with a nearly vertical nasal process, a very small prenarial portion and a large subnarial portion, neighboring anterior caudal vertebrae with a wide intervertebral space ventrally occupied by a knob-like chevron without a distal process, an ossified intervertebral disc between neighboring middle and posterior caudal vertebrae, furcular ramus with a constant width, a scapula with a rod-like acromion process, a dorsally curved and extremely thick blade, and an expanded mushroom-like distal end, a coracoid with an accessory foramen in scapular ramus, manual phalanges II-1 and III-2 with a proximodistally short but dorsoventrally deep proximal heel and a distal articulation with large semi-circular ventral hemicondyle and large collateral fossae, manual phalanx IV-1 much more robust than other manual phalanges, manual unguals with transversely expanded prominent flexor tubercle, fibular proximal end with a strongly concave medial edge and a robust posterior tuberosity, and about sixteen highly elongated tail feathers (about four times femoral length) near the end of bony tail.

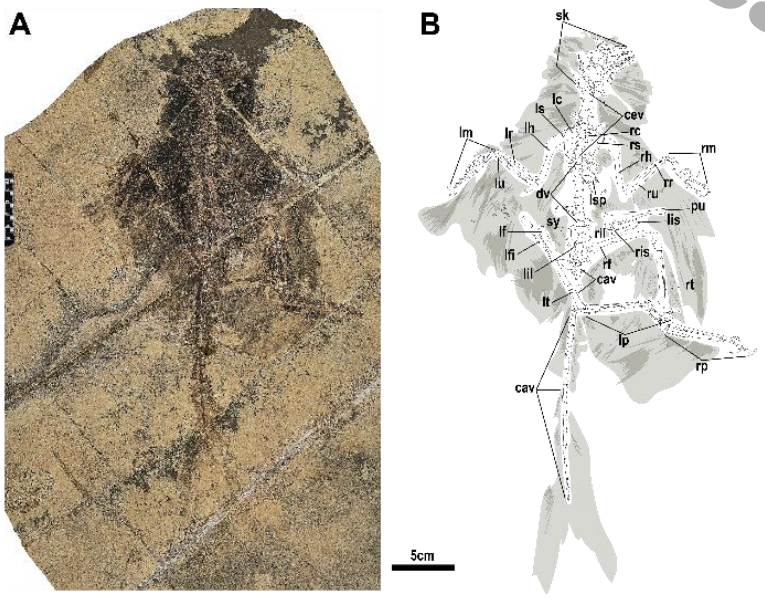

Fig. 1 Photograph (A) and line drawing (B) of *Changzhousaurus sinensis* holotype (LDNHMF 2026A)

Grey shadings indicate feathers. Abbreviations: cav, caudal vertebrae; cev, cervical vertebrae; dv, dorsal vertebrae; lc, left coracoid; lf, left femur; lh, left humerus; lis, left ischium; lm, left manus; lp, left pes; lr, left radius; ls, left scapula; lsp, left sternal plate; lu, left ulna; pu, pubis; rc, right coracoid; rf, right femur; rfi, right fibula; rh, right humerus; ril, right ilium; ris, right ischium; rm, right manus; rp, right pes; rr, right radius; rs, right scapula; rt, right tibiotarsus; ru, right ulna; sk, skull; sy, synsacrum

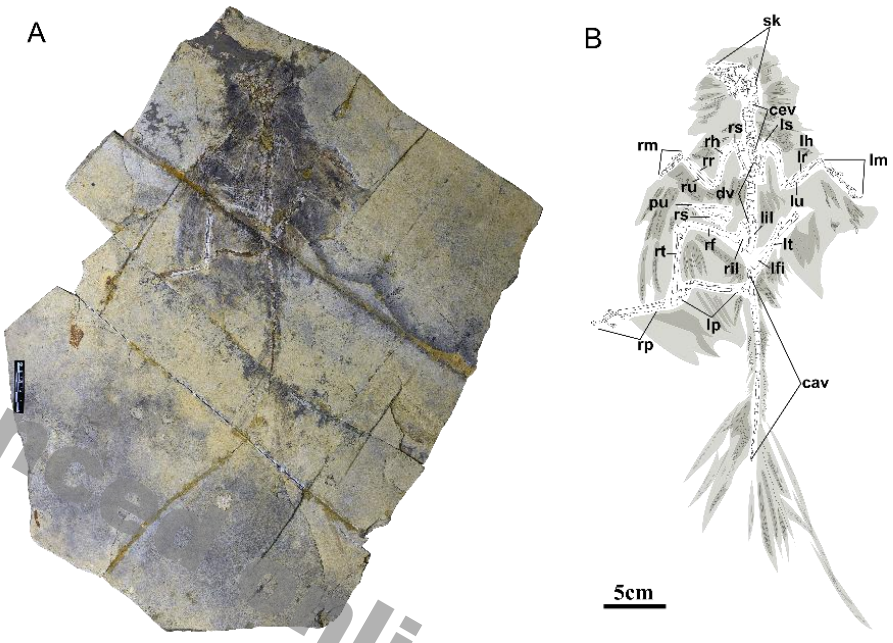

Fig. 2 Photograph (A) and line drawing (B) of *Changzhousaurus sinensis* holotype (LDNHMF 2026B)
Grey shadings indicate feathers. See Fig. 1 for abbreviations

3 Description and comparisons

The holotype is probably at subadult ontogenetic stage given that sacral vertebrae are fused to form a synsacrum, but proximal tarsals are not fused to each other and to tibia, and distal tarsals are not fused to metatarsals. The holotype measures ~340 millimeters in total skeletal body length, thus among the smallest known non-avialan theropods.

3.1 Cranial skeleton

The skull and mandible are mostly exposed on their lateral side, but the posterior cranial elements are either smashed or exposed on their dorsal side (Fig. 3). The skull is relatively small (estimated to have a skull-length/femur-length ratio of about 0.80), relatively deep in lateral view (with a ratio of pre-orbit bar height to skull length about 0.30), and with a relatively short snout (a length ratio of snout to skull about 0.5). The external naris is posterodorsally oriented (long axis about 35 degrees to the horizon) and is probably large in size. One fenestra is tentatively identified as the maxillary fenestra, which is very small in size, similar to the relatively small one seen in dromaeosaurids but unlike the large one in *Buitreraptor* and troodontids, and it is located away from the ventral border of the antorbital fossa, but not as dorsally displaced as in most dromaeosaurids (Makovicky et al., 2026).

The premaxilla has a nearly vertical anterior margin, a feature also seen in some troodontids such as *Byronosaurus* (Makovicky et al., 2003) and oviraptorosaurs (Osmólska et al., 2004), and a

convex ventral margin in lateral view. However, the nasal process is nearly vertically oriented, a feature only known in some oviraptorosaurs among pennaraptoran dinosaurs (Osmólska et al., 2004). The prenarial ramus is minimum in size and the subnarial ramus is large and sub-square in lateral view, a combination of features unknown in other paravians (Makovicky et al., 2026). The maxillary process is strap-like and orients posterodorally in lateral view.

The maxilla is deep in lateral view, and it displays a minimum anterior extension, with its anterior end considerably posterior to the anterior border of the external naris. In contrast, the maxilla extends anteriorly and overlaps the subnarial ramus of the premaxilla extensively in most troodontids (Makovicky et al., 2026). The antorbital fossa is poorly defined anteriorly and ventrally, and the possible interfenestra bar is flushed with the external surface of the maxilla as in *Byronosaurus* (Makovicky et al., 2003) and *Mei long* holotype. The floor of the antorbital fossa is smooth, without numerous pits and ridges as in the early-diverging dromaeosaurids microraptorines (Xu and Wu, 2001) and *Shanag* (Makovicky et al., 2026).

Fig. 3 Skull and mandible of *Changzhousaurus sinensis* holotype (LDNHMF 2026A)
Scale bar=1 cm

The lacrimal is somewhat T-shaped as in troodontids, dromaeosaurids, and some early-diverging avialans including *Archaeopteryx* (Makovicky et al., 2026). There is a right angle between anterior and descending processes but a larger angle between the latter and the posterior process. Both anterior and posterior processes are long, close in length to the descending process. For comparison, the posterior process is either absent or much shorter than the descending process in most theropods except ornithomimosaurs, dromaeosaurids, and troodontids. As in troodontids and the unenlagiinine *Austroraptor* (Novas et al., 2009), a prominent lateral flange seems to be present over orbital anterodorsal corner, and it is more similar to that of *Austroraptor* in a more posterior location. The nearly vertical descending process is relatively broad anteroposteriorly and bears a longitudinal groove, a feature seen in some microraptorines.

The postorbital is a tri-radiated element. The jugal process is long and slender, and displays a

distinctive anterior curvature, as in some troodontids such as *Sinovenator* (Xu, 2002), unlike the relatively short and robust one seen in most dromaeosaurids. The squamosal process is long, unlike the short one in *Austroraptor* (Novas et al., 2009), *Caihong* (Hu et al., 2018) and troodontids (Makovicky et al., 2026).

The quadrate shaft is strongly curved posteriorly so that there is an angle of about 130 degrees between the dorsal and ventral halves of the shaft. The relatively small pterygoid process is sub-triangular in outline, with a peak more ventrally located. The quadrate lacks a distinct flange near the quadrate ventral end for articulating the quadratojugal, and the lateral flange above the quadrate foramen is barely existent, both of which are known in dromaeosaurid quadrate (Makovicky et al., 2026)

The nasal appears to be long and narrow in dorsal view, but little other morphological details are preserved.

The frontal is large, and subtriangular in outline due to transversely very narrow anterior end and very wide posterior end as in most paravians (Makovicky et al., 2026). The orbital rim transits gradually to the postorbital process and it is dorsally deflected as in many early-diverging paravians (Makovicky et al., 2026). The posteromedial portion of the frontal is domed, though the compression during the fossilization minimizes the dome degree. The posterolateral portion appears to house the supratemporal fossa, which is well defined anteriorly and occupies a large portion of the frontal.

The parietal is fused to its counterpart. There is a sharp but low sagittal crest along the midline of the fused parietals. However, the sagittal crest terminates anterior to the posterior margin of the fused parietals. The nuchal crest is sigmoid in dorsal view, with a midline indentation. Prominent sagittal and nuchal crests are present in many dromaeosaurids, but not in oviraptorosaurs, troodontids and avialans (Makovicky et al., 2026)

The dentary is long and slender, with nearly parallel concave dorsal margin and convex ventral margin in lateral view, as in most dromaeosaurids (Makovicky et al., 2026). A groove is absent on the lateral surface of the anterior half of the dentary, though a row of foramina is present. Nevertheless, a broad groove appears to be present on the posterior half of the dentary, a feature known in many troodontids and the anchiornithine *Xiaotingia* (Xu et al., 2011).

Four teeth are present in each premaxilla. Their spatial distribution is identical to that seen in *Anchiornis* (IVPP V24456)(Wang et al., 2025): the interdental space is minimum between the first and second tooth, but wide between other premaxillary teeth. However, the first premaxillary tooth is more than one tooth position away from the anterior margin of the premaxilla, more distally located than in *Anchiornis* (V24456). The second tooth is the largest one of the four premaxillary teeth. All premaxillary teeth except the second one are nearly symmetrical in shape in lateral view, and the second one is slightly posteriorly curved. All premaxillary teeth lack serrations along both anterior and posterior carina.

Each maxilla bears about fifteen tooth sockets. The maxillary teeth are relatively sparsely distributed, with about a half tooth position between the neighboring teeth, and the interdental space is larger between anterior maxillary teeth than between posterior maxillary teeth. The middle maxillary teeth are larger in size than both anterior and posterior ones. Most maxillary teeth are nearly symmetrical in lateral view, but a few display slight posterior curvature. The crowns of most maxillary teeth lack a basal constriction in lateral view, but posterior ones have a slight constriction immediately below the crown. All preserved maxillary teeth lack serrations along either crown carina.

There are probably 20 tooth sockets in each dentary. As in some microraptorines such as *Microraptor* and many troodontids (Xu et al., 2000; Hwang et al., 2002), the anterior dentary teeth are slender and closely packed and posterior ones are relatively widely distributed and robust. The heterodonty is also indicated by the crown shape: anterior dentary teeth are slightly curved posteriorly and lack serrations along both anterior and posterior carina, but posterior dentary teeth display strong posterior curvature and bear posterior serrations, which are moderate in size and orient nearly perpendicular to the carina. The crown lingual surface of anterior dentary teeth is slightly concave or flat, with a distinct central ridge.

3.2 Postcranial skeleton

There are probably 10 cervical vertebrae (9 identifiable), 13 dorsal vertebrae, probably 6 sacral vertebrae, and 22 caudal vertebrae (Figs. 4-8). A low number of caudal vertebrae (fewer than 23) is also seen in most scansoriopterygids, some early-diverging oviraptorosaurs, and most avialans, while most other pennaraptorans have a larger number of caudal vertebrae (Makovicky et al., 2026).

The cervical vertebrae are mostly dorsally exposed (Fig. 4). They are wide transversely in dorsal view, with posterior ones even considerably wider than long (e.g., the ninth cervical vertebra has a maximum width:maximum length ratio of 1.8). The zygapophyses display strong lateral divergence particularly in posterior cervical vertebrae. Bump-like weak epipophyses are seen on dorsal surface of the postzygaphyses in posterior cervical vertebrae. The plate-like neural spines are long anteroposteriorly in most cervical vertebrae, but they are shorter in posterior cervical vertebrae, with the neural spine of the posteriomost cervical minimum in anteroposterior length.

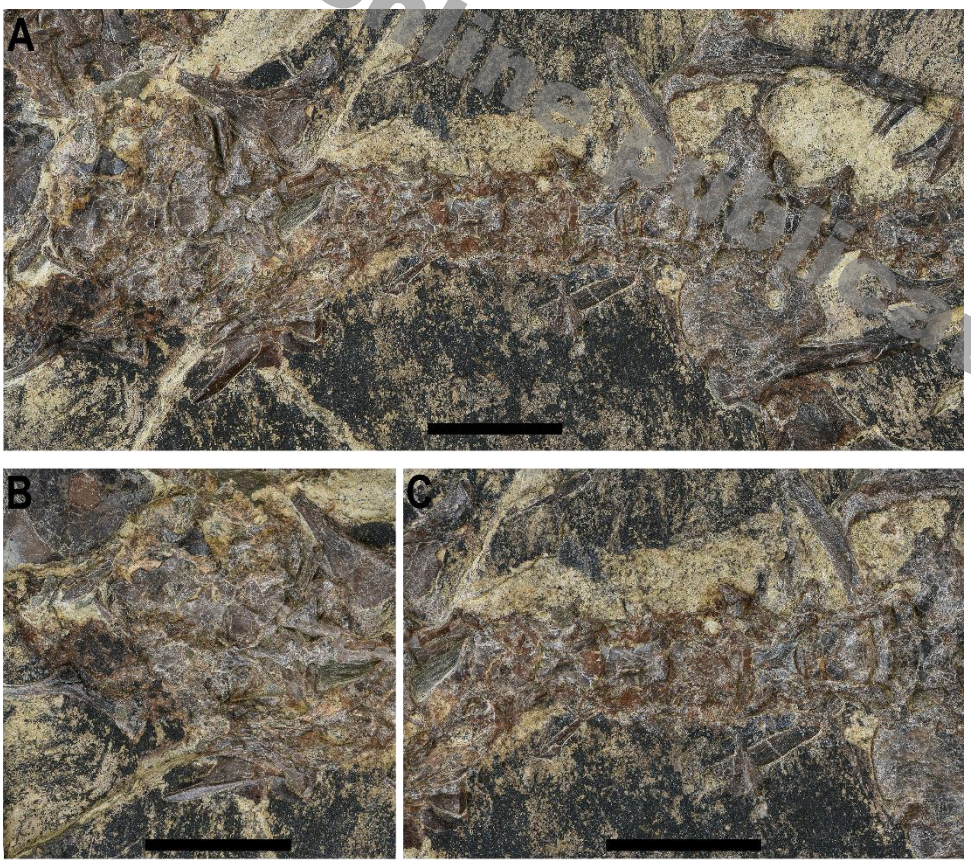

Fig. 4 Cervical vertebrae of *Changzhousaurus sinensis* holotype (LDNHMF 2026A)
A. cervical series; B. anterior cervical vertebrae; C. posterior cervical vertebrae. Scale bars=1 cm

Several cervical ribs are visible on the slab. The anterior ones are slightly longer than the corresponding cervical vertebrae, and they are slender in lateral view. The posterior cervical ribs are about the length of the corresponding cervical vertebrae, and they are robust and with a somewhat triangular shape in lateral view.

Most dorsal vertebrae are laterally exposed on the slab (Fig. 6). Anterior dorsal vertebrae are distinctly shorter than middle and posterior ones in lateral view, and distinct pneumatic openings are not seen in any dorsal vertebra, though anteriormost dorsal vertebrae expose only their dorsal side. Unusually, anterior six dorsal vertebrae all seem to have angled centra, with anterior and posterior articular surfaces not perpendicular to the central ventral margin in lateral view. More posterior dorsal vertebrae have elongated and sub-rectangular centra (about twice as long as tall) as in most small-sized theropods (Makovicky et al., 2026).

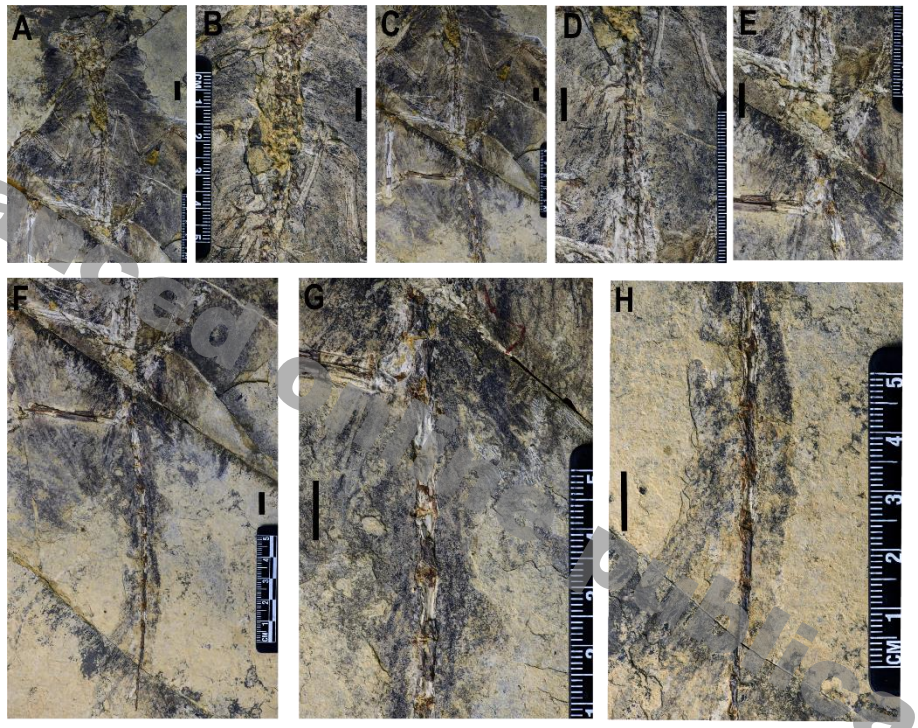

Fig. 5 Vertebral column of *Changzhousaurus sinensis* holotype (LDNHMF 2026B)
A. cervical, dorsal, and sacral series; B. posterior cervical vertebrae and anterior dorsal vertebrae; C. dorsal series, sacral series, and anterior caudal vertebrae; D. dorsal series; E. Sacral series and anterior caudal vertebrae; F. caudal series; G. anteromiddle caudal vertebrae; H. posterior caudal vertebrae. Scale bars=1 cm

Sixteen dorsal ribs are visible on the slab. The visible longest dorsal rib, which is associated with anterior dorsal vertebrae, is 17.7 mm in length; and the shortest one is 7.9 mm in length, which attaches to the second last dorsal vertebra. In general, the dorsal ribs seem to be proportionally short, for example, the preserved longest rib is about 40% of the femoral length, compared to about 60% in some microraptorines (e.g., IVPP V23490). Dorsal ribs are curved but are relatively straight along the distal part of the rib shaft. The capitular process, which is largely aligned with the rib shaft, is short and robust, and the tubercular process is long and slender and distally expanded to form the articular facet for the corresponding dorsal vertebra. There is a distinct ridge, emanating from the joint region of the capitular and tubercular processes along the rib medial surface, and posterior to the ridge is a parallel groove. In anterior dorsal ribs, the capitulum and tuberculum

are widely separated, and the capitular process is relatively long and slender. The proximal end of the anterior dorsal ribs seems to be proportionally wide, with a capitular flange. In more posterior dorsal ribs, the capitulum and tuberculum are less widely separated from each other, with the capitular process shorter and more robust. The capitular processes of the posteriormost ribs are minimum in size and they are more like a triangular projection rather than a distinct process.

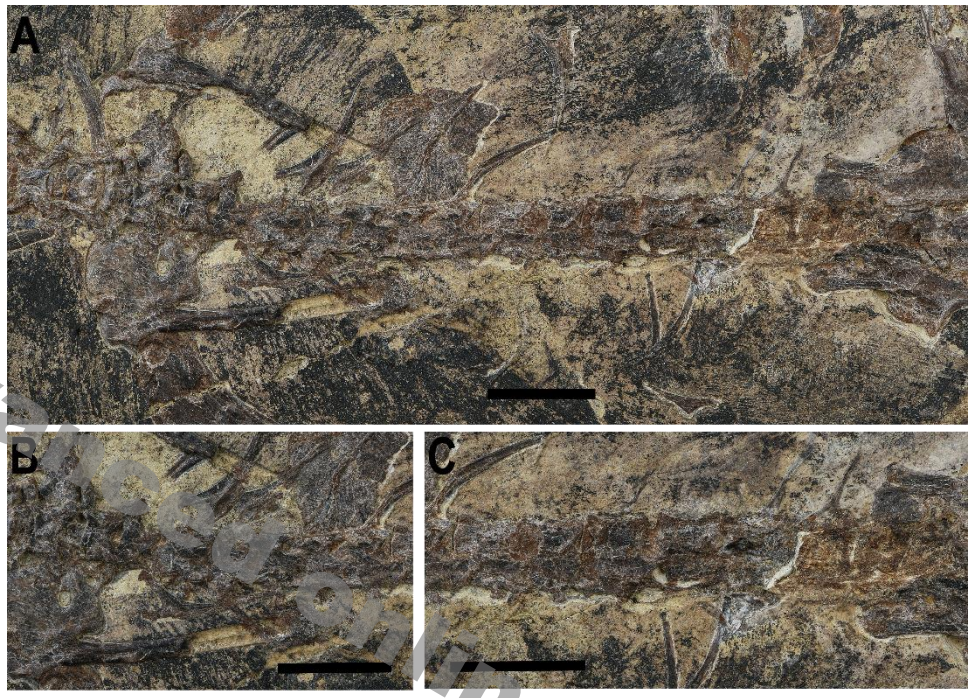

Fig. 6 Dorsal vertebrae of *Changzhousaurus sinensis* holotype (LDNHMF 2026A)
A. dorsal series; B. anterior dorsal vertebrae; C. posterior vertebrae. Scale bars=1 cm

Several small rod-like bones are visible on the slab, and they are identified as gastralia rather than uncinate processes. The latter are absent in some pennaraptorans such as *Archaeopteryx* (Mayr et al., 2005) and *Anchiornis* (Makovicky et al., 2026).

One sternal plate is partially visible on the slab (Fig. 1), and it might be the posterior half of the left sternal plate. The preserved portion of the sternal plate suggests that it is much longer than wide. The preserved lateral margin lack the sternal rib articulations separated by notches (Makovicky et al., 2026), suggesting that the sternal rib articulations are restricted to the anterior portion of the sternal plate and the sternal ribs are low in numbers; alternatively, the articular facets for the sternal rib are cartilaginous. The posterior half of the sternal lateral margin flares laterally and the posterior margin is convex, and thus the midline of the posterior margin of the paired sternal plates is strongly indented. Ossified sternum is known in most pennaraptorans but not in *Archaeopteryx, Sapeornis*, anchiornithines, or troodontids (O'Connor et al., 2015).

The synsacrum is 26.5 mm long, formed by probably 6 sacral vertebrae, one dorsal vertebra, and one caudal vertebra (Fig. 7). The last dorsal vertebra is placed between the two ilia, but little morphological data is available. In dorsal view, the neural arches including the neural spines of the sacral vertebrae are completely fused to each other, forming a continuous neural-spine plate and two flat neural-arch shelves lateral to the fused neural spine. There is a round fenestra between the posterolaterally oriented and distally wider fifth sacral rib-transverse process compound and the

preceding compound. The sixth sacral rib-transverse process compound is about twice the corresponding centrum length, considerably longer than the preceding one, suggesting that the posterior end of the ilium is diverged laterally. The compounds all have a narrower base and broader distal end in dorsal view, and they shift their position on the corresponding centrum from near anterior central articular end to near posterior central articular end.

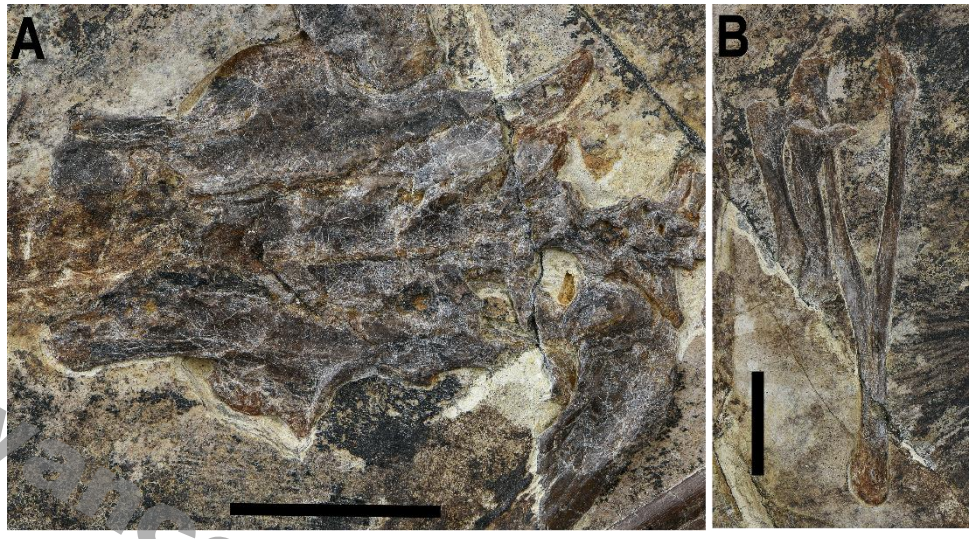

Fig. 7 Synsacrum and pelvic girdle of *Changzhousaurus sinensis* holotype (LDNHMF 2026A)
A. sacral series and two ilia; B. pubes and ischia. Scale bars=1 cm

There are 22 caudal vertebrae. Anterior six caudal vertebrae are dorsally or obliquely exposed and the remaining caudal vertebrae are laterally exposed on the slab (Figs. 1, 2, 8). The caudal series is relatively short, 3.4 times as long as the femur, and as in other paravians, there is a transitional point in caudal series (Makovicky et al., 2026). Seven anterior caudal vertebrae display a gradual increase in anteroposterior length, and the eighth caudal vertebra shows a significant increase in length, with caudal vertebrae 8-17 being about the same anteroposterior length, and the eighteenth one displays a significant decrease in length and the decrease continues to the last caudal vertebra. The middle caudal vertebrae are more than twice as long as the middle dorsal vertebrae and are slender in lateral view (e.g., a middle caudal vertebra is more than five times as long as deep in lateral view). The neural spine and transverse processes are absent in caudal 8 and more posterior caudal vertebrae, and they are likely to be absent in some more anterior caudal vertebrae. The caudal transitional point is thus positioned at least anterior to caudal 8.

Caudal vertebra 1 is fused to the last sacral vertebra. Its centrum is much wider than long in dorsal view and the centrum posterior articular surface is semi-circular in outline with a transverse width:dorsoventral height ratio of greater than 2.0. The strap-like transverse process is about the centum length and has a blunt distal end unlike the distally tapered one seen in early-diverging troodontids such as *Sinovenator* and the anchiornines such as *Xiaotingia*, and it is located close to the posterior end of the centrum and orients posterolaterally (Makovicky et al., 2026). Caudal vertebrae 2 and 3 appear to be similar in general morphology to caudal vertebra 1. Caudal vertebra 4 is different from caudal vertebrae 1-3 in having laterally oriented and distally expanded transverse processes (expanding in posterior direction), and the transverse process is considerably longer than the centrum. The transverse processes of Caudal 5 vertebra are slender, distally tapered, positioned more anteriorly on the centrum, and anterolaterally oriented.

More posterior caudal vertebrae display amphiplatyan central articular surfaces and highly elongated centra in lateral view. There is a distinct broad longitudinal depression on the central lateral surface. The zygapophyses are short, with the prezygapophyses covering less than one-fourth of the length of the preceding vertebra and the postzygaophyses are minimum. Unusually, ossified intervertebral discs are preserved between the neighboring middle and posterior caudal vertebrae.

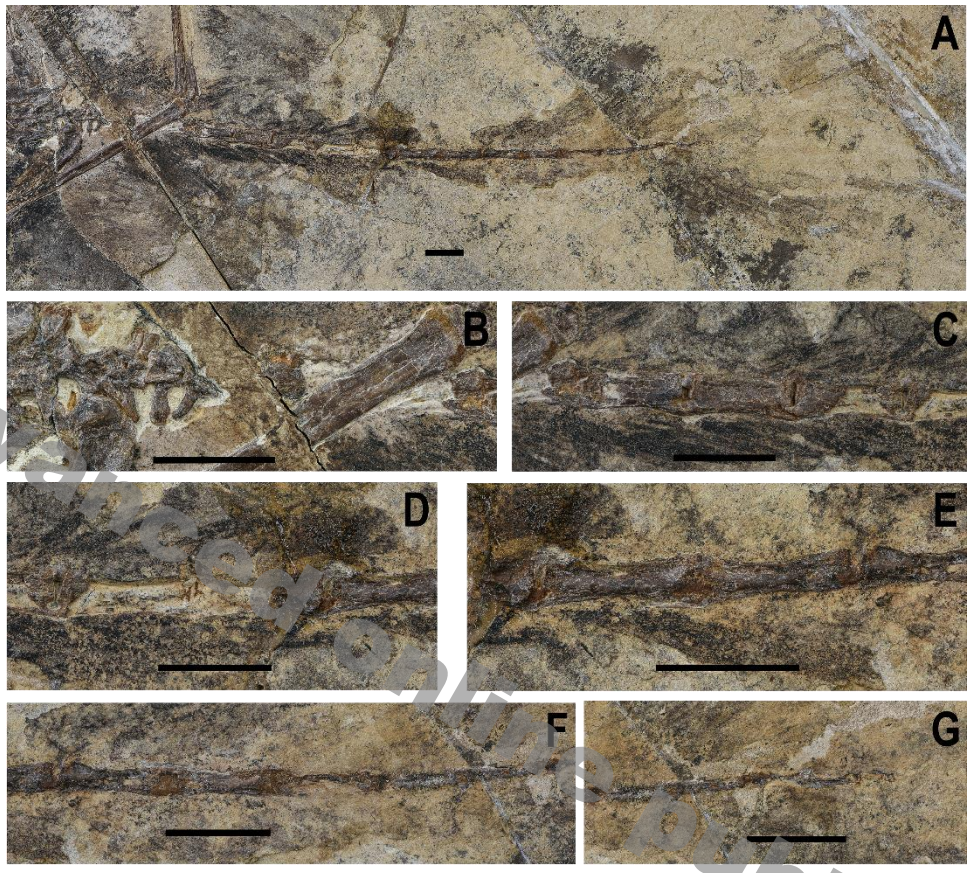

Fig. 8 Caudal vertebrae of *Changzhousaurus sinensis* holotype (LDNHMF 2026A)

A. caudal series; B. anteriormost caudal vertebrae; C. anteromiddle caudal vertebrae; D. middle caudal vertebrae; E. postomiddle caudal vertebrae; F. posterior caudal vertebrae; G. posteriormost caudal vertebrae. Scale bars=1 cm

The visible chevrons are preserved associated with caudal vertebra 9 and more posterior ones. In general, they are all extremely small compared to the associated caudal vertebrae but display some variations. The anterior two chevrons are knob-like structures located between the centra of two neighboring caudal vertebrae, with the posterior one of the two being 1.3 mm long and 1.0 mm tall (for comparison, the anterior articular surface of the associated caudal centrum is 2.8 mm in height). More posterior chevrons bear small anterior and posterior extensions, thus producing somewhat an inverted T-like shape in lateral view, and the posterior extension is longer than anterior one in posterior chevrons. The proportionally longest chevon is about 25% of the associated caudal length. Middle and posterior chevrons have transversely convex ventral surface, and they are also slightly bowed ventrally, unlike the long and flat ones seen in many other paravians (Makovicky et al., 2026). Anteroposteriorly short and ventrally convex chevrons in lateral view are also seen in *Makahala*, *Anchiornis*, and *Archaeopteryx* (Makovicky et al., 2026).

The scapula is relatively short (Figs. 9, 10), with a scapula:femur length ratio of 0.59. As in many paravians (Makovicky et al., 2026), it is nearly parallel to the axial column. The smooth

proximal articular surface of the scapula suggests a mobile articulation with the coracoid. The scapular acromion process has little dorsal expansion but a moderate anterior extension. The acromion process is robust and somewhat rod-like (mediolaterally wider than dorsoventrally deep), with a gap from the articular facet for the coracoid, suggesting the presence of a foramen triosseum. It is laterally strongly everted to roof a groove on scapular lateral surface near the proximal end. The glenoid fossa is located on the scapular ventral surface and the scapular contribution to the glenoid fossa is much larger than the coracoidal contribution. The scapular blade is curved dorsally and slightly medially. It is slender in lateral view and relatively thick mediolaterally. The narrowest part of the scapular blade lies near its mid-length, not at the proximal or distal region. Distally the scapular blade widens gradually and near the distal end, it is abruptly expanded and with a strongly convex distal margin, forming a somewhat mushroom-like structure, with a width greater than 150% of scapular blade minimum width.

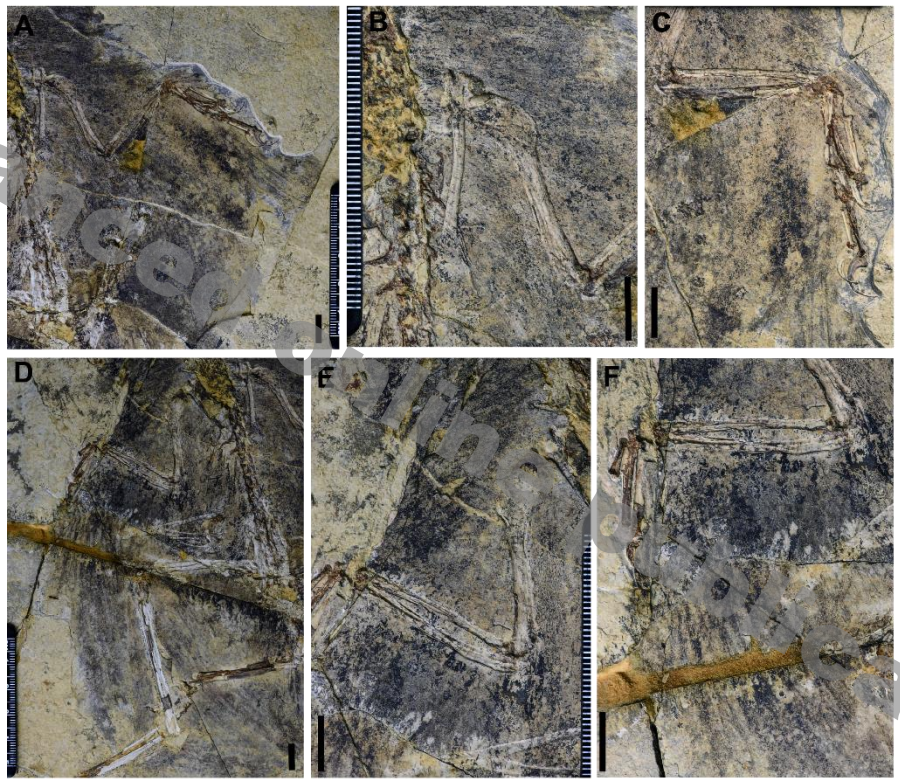

Fig. 9 Pectoral girdle and forelimbs of *Changzhousaurus sinensis* holotype (LDNHMF 2026A)

A. left pectoral girdle and forelimb; B. left scapula and coracoid; C. left humerus; D. left ulna and radius; E. left manus; F. right pectoral girdle and forelimb; G. right scapula and coracoid; H. right humerus; I. right ulna and radius; J. right manus. Scale bars=1 cm

The coracoid is a proportionally large rectangular plate (Figs. 9,10), but it is essentially a bi-ramus structure comprising a proximal ramus (i.e., scapular ramus) and a distal ramus (i.e., sternal ramus) as in other maniraptoriforms (Xu et al., 2013). The border between the scapular ramus and sternal ramus emanates from the coracoid tubercle, which is sharply pointed. The coracoid tubercle is positioned along lateral margin and laterally projected as in unenlagiinies, *Archaeopteryx* (Wellnhofer, 2009), and *Sapeornis*. The border is not distinct, but it can be inferred to have an angle with the lateral margin (posterior margin) of the sternal ramus about 90 degrees as in many early-diverging pennaraptorans, leading to an L-shaped coracoid in lateral view as in many maniraptorans

(Xu et al., 2002; Xu et al., 2013). In some pennaraptorans such as late-diverging troodontids, the coracoid is more plate-like rather than being inflected (Makovicky et al., 2026). The scapular ramus is sub-equal in size to the sternal ramus. It bears a restricted articular surface for the scapula, medial to which is a large concavity. This concavity is bound more medially by a separate process, which is probably homologous to the procoracoid process. A distinct procoracoid process is absent in the earliest-diverging avialans such as *Archaeopteryx* and *Sapeornis* as indicated by the straight proximal margin of the coracoid in these taxa, and it is only known among later-diverging Avialae. The coracoid foramen (supracoracoid foramen in some literature) is hypertrophied and there is an accessory foramen medial (dorsal) to the coracoid foramen. The sternal ramus lacks a fenestra as in most Jehol dromaeosaurids except *Tianyuraptor* and *Zhengyuanlong* (Zheng et al., 2010; Lu and Brusatte, 2015), but it has a large shallow fossa on the medial/posterior surface, which is also present in some dromaeosaurids such as *Deinonychus* and possibly *Archaeopteryx* (Ostrom, 1969; Xu et al., 2011). The lateral margin of the sternal ramus is concave, the anterior margin is slightly convex, and the medial margin is straight.

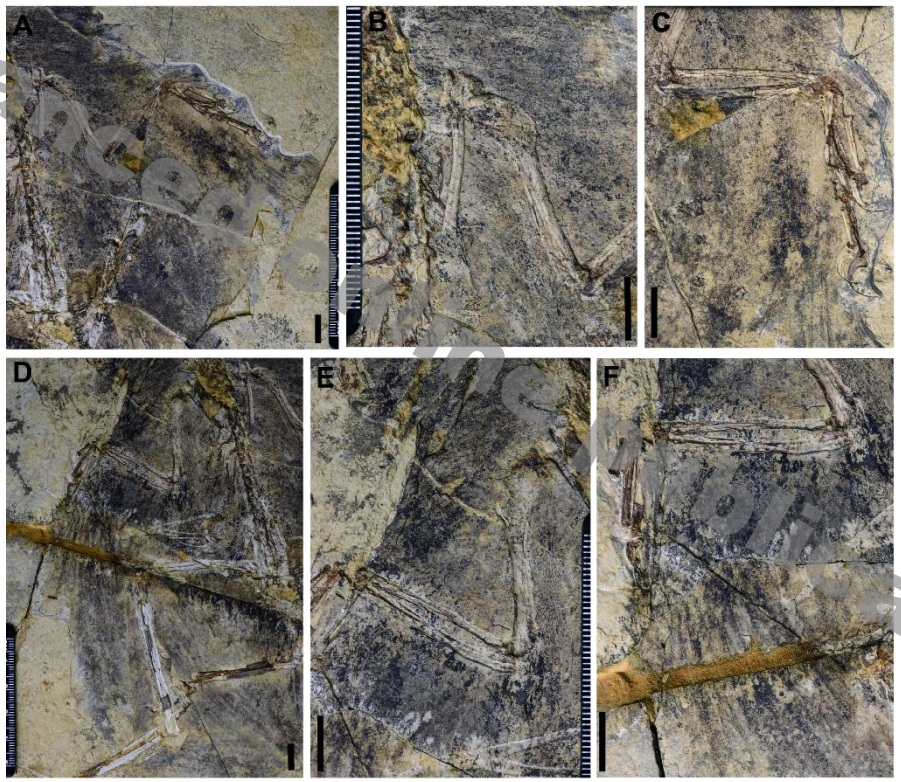

Fig. 10 Pectoral girdle and forelimbs of *Changzhousaurus sinensis* holotype (LDNHMF 2026B)

A. left pectoral girdle and forelimb; B. left pectoral girdle and left humerus; C. left forearm; D. right pectoral girdle and forelimb; E. right humerus, ulna, and radius; F. right ulna, radius, and manus. Scale bars=1 cm

The furcula is anteroposteriorly flattened and boomerang-shaped as in many pennaraptorans including early-diverging avialans such as *Archaeopteryx* and *Confuciusornis* (Makovicky et al., 2026). It has a transverse width of 22.5 mm and an inter-clavicular angle of about 90 degrees. The omal (epicleidal) end of the furcula seems to be simple in morphology, unlike the twisted one seen in early-diverging avialans such as *Archaeopteryx* and *Xiaotingia* (Xu et al., 2011). The clavicular ramus is much narrower than the proximal portion of the scapular blade, and it remains about the same width throughout the length, whereas in most other pennaraptorans, the clavicular ramus is

wider toward the inter-clavicular region (Makovicky et al., 2026).

The forelimb is relatively long, about 60% of the hindlimb length (Figs. 1, 2). The forelimb proportion is similar to that of some early-diverging paravians such as in *Xiaotingia*: the radius and manus are about 95% and 115% of the humeral length, respectively, compared to 90% and 115% in *Xiaotingia*; while in *Microraptor* (e.g., IVPP V13352), these proportions are about 85% and 130%. Proportionally long manus is seen in many other early-diverging pennaraptorans (Makovicky et al., 2026). As preserved, the forearm forms an angle of about 75 degrees with the humerus, and of about 90 degrees with the manus, the latter often seen in early-diverging paravians such as *Archaeopteryx*, *Microraptor*, and *Mei* (Makovicky et al., 2026)

The humerus is about 75% of the femoral length, and it is about the same thickness as the latter. The humeral head is slightly offset from shaft, and it is an obliquely oriented crest-like structure overhanging the posterior surface (Figs. 9, 10). The internal tuberosity is elongated as in early-diverging paravians (Makovicky et al., 2026), and it is more distally located than the humeral head. The humeral deltopectrol crest is about 40 % of the humeral length, and it bears a depression on the distal portion of the posterior surface. For comparison, the deltopectoral crest is much shorter in anchiornithines (Pei et al., 2017) and some microraptorines such as *Graciliraptor* (Xu and Wang, 2004). The distal end is wide (about 1.5 times as wide as the mid-shaft), strongly twisted relative to the proximal end, and bears prominent radial and ulnar condyles on the anterior surface.

The ulna is considerably thinner than the humerus (Figs. 9, 10). Proximally, it has a proximally rounded olecranon process. The shaft is distinctly bowed posteriorly as in most paravians, whereas in anchiornithines except *Xiaotingia* and some troodontids, it is nearly straight (Makovicky et al., 2026).

The radius is bowed anteriorly, and with the posteriorly bowed ulna, form a relatively broad forearm (Figs. 9, 10), a derived feature only known in *Xiaotingia* (STM 27-2) and possibly also in unenlagiinine *Buitreraptor* (Gianechini et al., 2018). The radius is relatively thick, only slightly thinner than the ulna as in in troodontids and anchiornithines, while in most other paravians the radius is distinctly thinner than the ulna (Makovicky et al., 2026). The distal end of the radius is little expanded.

There are at least three free carpals: a large proximal carpal near the distal end of the ulna, a large distal carpal primarily contacting the proximal end of metacarpal III, and a small distal carpal contacting the proximal ends of both metacarpals III and IV. The large distal carpal, identified as the 'semilunate' carpal, is strongly convex proximally in dorsal view, and it has a proximodistal to transverse length ratio of about 0.70, greater than in most other early-diverging paravians. The small distal carpal is identified as the distal carpal 4, and it attaches to the laterodistal corner of the 'semilunate' carpal as in some early-diverging deinonychosaurian specimens such as *Mei long* holotype (Xu et al., 2014b). The large proximal carpal, identified as ulnare, is even larger in size than the 'semilunate' carpal and appears to be V-shaped as in late-diverging birds (Napoli et al., 2025), though the preservation makes it difficult to confirm this morphological observation.

Metacarpals are similar in general morphology to those of *Xiaotingia*: Metacarpal II is about 30% of metacarpal III length, metacarpal IV is laterally bowed, about the same in robustness as metacarpal III, and slightly longer than the latter. Proportionally long and robust metacarpal IV is also seen in scansoriopterygids, halszkaraptorines, *Mei*, and many enantiornithines (Makovicky et al., 2026), and but it is nearly straight in these taxa.

The manus comprises a relatively long manual digit II (extending distally considerably beyond

the distal end of metacarpal III) and a long manual digit IV similar in length to manual digit IV. Elongate manual digit IV is also known in scansoriopterygids, halszkaraptorines, and *Mei* (Makovicky et al., 2026). Manual phalanx II-1 is about 80% the length of metacarpal III, and in lateral view it is slightly curved ventrally. It possesses a proximoventral heel on the proximal end and a proximodistally elongated distal articulation. The distal end is little expanded dorsally but strongly expanded ventrally, and bears a large medial collateral ligmental fossa, similar features also present in two other penultimate manual phalanges (i.e., manual phalanges III-2 and IV-3). Manual phalanx III-1 is robust and with a proximodistally short distal end. Manual phalanx III-2 is much longer than III-1, with an III-2:III-1 length ratio of 1.86, and it is also slightly curved ventrally similar to II-1. Manual phalanx IV-1 is much more robust than other phalanges including III-1. Manual phalanx IV-2 is short, about 60% of the length of III-1, a feature also seen in dromaeosaurids and *Archaeopteryx* (Xu et al., 2011) and it bears a proximoventral heel. Manual phalanx IV-3 is long relative to metacarpal III (an IV-3:MC III length ratio of 0.77), and it is straight in lateral view.

The manual unguals are all strongly curved and dorsally arched (the dorsal margin considerably dorsal to the proximal end when the proximal articular facet is held vertical), are robust in lateral view, and bears a proximodorsal lip and a medially (probably also laterally) expanded flexor tubercle located considerably distal to proximal articular surface. Manual ungual II is the largest one of the three unguals (about 120% manual ungual III length). Manual ungual IV is relatively large (93% of manual ungual III length), proportionally larger than in most other early-diverging maniraptoran dinosaurs.

The ilium is small, with an ilium-to-femur length ratio of 0.54, as in most Jehol dromaeosaurids and many other early-diverging paravians. The ilium is shallow in lateral view (Fig. 7), with the acetabulum-level height to the anteroposterior length ratio of 0.18, compared to 0.17 in *Xiaotingia*, 0.23 in *Anchiornis* (IVPP V23489), and 0.15 in *Rahonavis* (Forster et al., 2020), and its dorsal margin is slightly convex in lateral view as in *Rahonavis* (Forster et al., 2020). The preacetabular process is much longer than the postacetabular process as in many early-diverging paravian and scansoriopterygids, and it is shallow in lateral view as in *Rahonavis* (Forster et al., 2020) and some early-diverging avialans such as *Archaeopteryx* (Wellnhofer, 2009). It has a slightly convex anterior margin in lateral view unlike the strongly convex one in scansoriopterygids, unenlagiines and early-diverging avialans. A distinct anteroventral process is absent as in *Archaeopteryx* (Wellnhofer, 2009), whereas in most other early-diverging pennaraptorans including anchiornithines, unenlagiines and some early-diverging avialans such as *Sapeornis*, there is a distinct iliac anterovenral process and in the latter two groups, it is posteriorly located. The pubic peduncle is large, with the anteroposterior length about 25% of the iliac length, compared to about 20% in *Rahonavis* (Forster et al., 2020), about 30% in *Xiaotingia*, and 15% in *Anchiornis*. The pubic peduncle is proportionally wide in lateral view, about 2.4 times as wide anteroposteriorly as high dorsoventrally measuring at the mid-length of the peduncle, compared to about 2.2 in *Xiaotingia*, 3.1 in *Rahonavis* (Forster et al., 2020), and 1.4 in *Anchiornis*. As in many early-diverging paravians, most of the lateral surface of the pubic peduncle is depressed to form the cuppedicus fossa, which is bound dorsally by a nearly horizontally oriented thick ridge. The cuppedicus fossa has a large lateral exposure below the preacetabular process as in unenlagiines, early-diverging dromaeosaurids, some early-diverging avialans such as *Sapeornis*, and the anchiornithine *Xiaotingia*, but in some other early-diverging paravians such as *Anchiornis*, *Archaeopteryx*, and early-diverging troodontids including *Sinovenator*, it has limited lateral exposure below the preacetabular process (Hwang et al., 2002; Xu, 2002; Pei et al., 2017;

Gianechini et al., 2018; Forster et al., 2020). As in anchiornithines and early-diverging dromaeosaurids (Makovicky et al., 2026), the pubic peduncle bears a distinct concave ventral margin in lateral view. The ischial peduncle is extremely small, and its long axis is posteroventrally oriented, and thus making a sharp angle with the ventral margin of the postacetabular process. Posteroventrally oriented ischial peduncle is also known in some microraptorines, but in most other pennaraptorans, the peduncle is ventrally oriented. There is a ball-like antitrochanter located relatively dorsally. The supracetabular crest is present only along the anterior half of the acetabular rim as in *Hesperonychus* and *Unenlagiia* (Longrich and Currie, 2009), unlike the fully developed one in *Anchiornis* and *Rahonavis* (Makovicky et al., 2026). The postacetabular process is shallow, tapered posteriorly, curved ventrally to the level of ischial peduncle ventral margin in lateral view as in many dromaeosaurids including *Mahakala*, unenlagiines and microraptorines (Makovicky et al., 2026)

The pubis is long, measuring 88% of the femoral length (Fig. 7). In posterior view, the pubic shaft is nearly straight for most length except the ventral third where it is slightly concave medially. The proximal end comprises an extremely short ischial peduncle with a relatively long articular facet for the ischium and an iliac peduncle that is wide in lateral view. A pubic apron ridge emanates near the distal margin of the ischial peduncle along the medial surface of the pubic shaft as in *Rahonavis* (Forster et al., 2020), though it emanates slightly more distally in the latter taxon, whereas in *Sinovenator* it emanates considerably more distally and along the posterior edge of the pubic shaft. Distally the ridge becomes prominent and shifts to the anterior edge of the pubic shaft forming with its counterpart a pubic apron. The pubic apron is mediolaterally narrow (a ratio of apron width to pubic length less than 0.05) and is relatively short (slightly less than 50% of the pubic length). Distally the pubis appears to be spatulate in lateral view, without a distinct pubic boot as in microraptorines and early-diverging troodontids such as *Sinovenator* (Makovicky et al., 2026).

The ischium is a slender and strap-like bone (Fig. 7) as in some microraptorines and *Xiaotingia* (Xu et al., 2011). The pubic peduncle is long and slender in lateral view, with the articular surface medially inclined. It sets an angle of about 100 degrees to the ischial shaft, with a flat lateral surface and a convex medial surface. The short and robust iliac peduncle is aligned with the ischial shaft, and it is more knob-like (strongly expanded laterally and with its articular surface laterally exposed). These features are also seen in some microraptorines but absent in most other pennaraptorians. In latter taxa, the pubic and ischial peduncles are similar in size and forked from the ischial shaft at about the same angle. The anterior margin of the ischial shaft is strongly thickened as in some microraptorines, but lack a longitudinal groove seen in the latter. The majority of the ischial shaft is thin, though the lateral surface is concave as in many troodontids. Along the posterior margin are two extremely small processes, one located close to the proximal end and one more distally. The distal one-third of ischial shaft is slightly curved posteriorly. As preserved, the distal end bears a robust rectangular obturator process that is distally oriented and a small posterodistal process, and they are separated by a notch. These features are also present in *Archaeopteryx* (Wellnhofer, 2009). The ischia are unfused distally as in other pennaraptorans (Makovicky et al., 2026)

The femur is an anteriorly bowed bone (Figs. 11, 12). The ball-like femoral head orients medially and is higher than the trochanteric crest. It lacks a distinct neck separating from the latter. The greater trochanter is wide anteroposteriorly and separates from the lessor trochanter by a small notch. The lessor trochanter extends proximally to the level of the greater trochanter but is positioned medial to the latter. The trochanteric shelf is relatively proximally and centrally located.

There is an accessory crest at the base of lesser trochanter, albeit small in size. A small posterior trochanter is located along the boundary of lateral and posterior surfaces near the femoral proximal end as in other paravians (Makovicky et al., 2026). Distally, there is a distinctive intercondylar groove on the anterior surface of the femoral distal end.

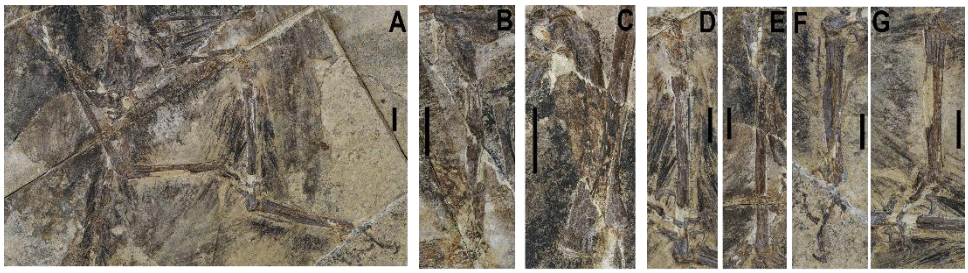

Fig. 11 Hindlimbs of *Changzhousaurus sinensis* holotype (LDNHMF 2026A)

A. left and right hindlimbs; B. right femur; C. left femur, tibia, and fibula; D. right tibia and fibula; E. left tibia and fibula; F. right pes; G. left pes. Scale bars=1 cm

The tibia measures about 125% of the femoral length. The proximal end is only slightly expanded mediolaterally, and its articular surface is higher anteriorly than posteriorly (Figs. 11, 12). It has a slightly curved shaft and a little expanded distal end as in many early-diverging paravians (Makovicky et al., 2026).

The fibula is long, extending distally to contact the calcaneum (Figs. 11, 12). The proximal end has a concave medial margin in proximal view, and its posterior margin is thickened mediolaterally and expands posteriorly to form a ball-like structure, which is unknown in other theropods. There is a longitudinal depression on anterior half of the medial surface near proximal end. The fibula shaft is rod-like rather than strap-like as in some anchiornithines.

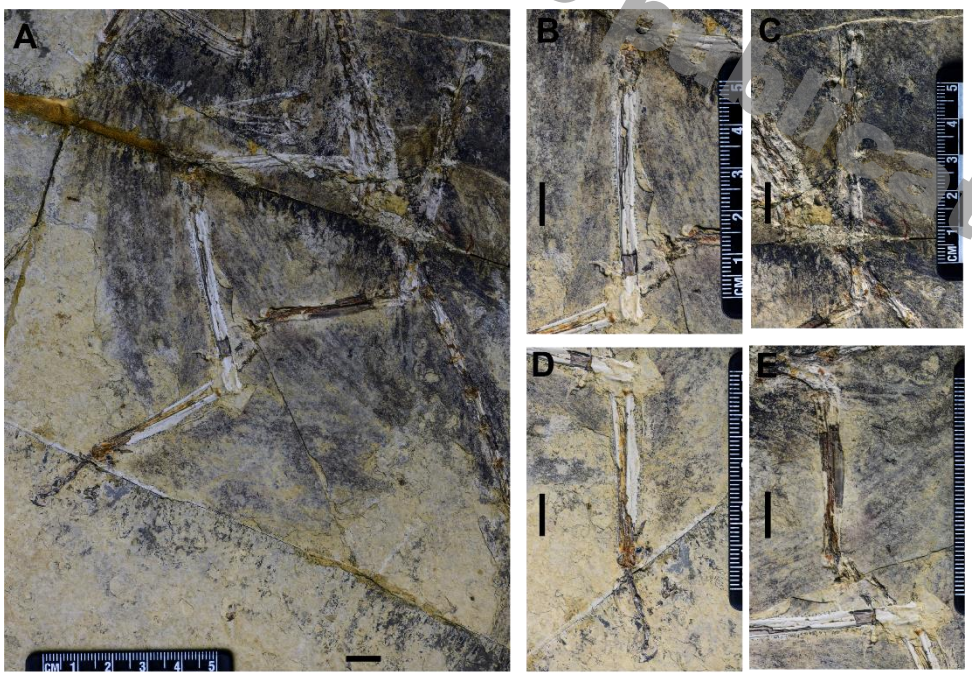

Fig. 12 Hindlimbs of *Changzhousaurus sinensis* holotype (LDNHMF 2026B)

A. left hindlimb; B. left tibia and fibula; C. right tibia and fibula; D. right pes; E. left pes. Scale bars=1 cm

The astragalus and calcaneum are not fused to the tibia (Figs. 11, 12). The right calcaneum is partially fused to the astragalus, but the left one is separate from the left astragalus. The disc-like calcaneum has a concave lateral surface, and it contributes a very small portion of the articular surface. The astragalus has a larger medial condyle, which is separated from the lateral one by a distinct groove on the distal surface.

Two distal tarsals are present, and they are not fused to the metatarsals. Both are thin disc-like bones and are identified as distal tarsals III and IV based on their topological position.

In general, pedal digits are relatively short (e.g., a length ratio of III-1+2+3 to metatarsal III being about 0.50), similar in relative length to those of troodontids and dromaeosaurids but shorter than those of some other early-diverging paravians (e.g., about 0.60 in *Anchiornis* and 0.80 in *Archaeopteryx*). Pedal digit I is very small in size (the ratio of combined lengths of metatarsal I, phalanx I-1, and phalanx I-2 to the length of metatarsal III is about 0.2, compared to about 0.4 in *Anchiornis* V23487 and 0.35 in *Sinovenator* IVPP V12618), and it terminates well proximal to the distal end of metatarsal III, while in many early-diverging paravians including the troodontid *Sinovenator*, it extends more distally, at least to the level of metatarsal III distal end. Pedal digit II is modified, with an enlarged ungual as in troodontids and dromaeosaurids. Pedal digit III is distinctly longer than other pedal digits including pedal digit IV, which terminates about the level of the proximal end of pedal phalanx III-4. For comparison, pedal digit IV extends more distally in most early-diverging paravians, and in troodontids and dromaeosaurids, digit IV is subequal to digit III in length (Makovicky et al., 2026).

Metatarsal I is only 8% as long as metatarsal III, compared to 16% in the microraptorine *Sinornithosaurus* (. Metatarsal II measures about 90% of metatarsal III length; metatarsal IV is nearly as long as metatarsal III and is much wider than other metatarsals. Such an asymmetric metatarsus is also seen in troodontids and to a lesser degree in some dromaeosaurids (Xu and Wang, 2000). Metatarsal II has a distal end sub-equal in transverse width to that of metatarsal III. A slender, short metatarsal II is a troodontid feature (Makovicky and Norell, 2004). In posterior view, the proximal end of metatarsal III is about half as wide as that of metatarsal II, which is considerably narrower than that of metatarsal IV. Proximally narrow metatarsal III is also seen in early-diverging dromaeosaurids such as microraptorines, unenlagiines (Makovicky et al., 2005; Novas and Pol, 2005; Novas et al., 2018), and early-diverging troodontids. The distal articulation of metatarsal III appears not to be ginglymoid. A ginglymoid one is seen in many early-diverging avialans (Chiappe and Walker, 2002), and to a lesser degree in some dromaeosaurids and troodontids (Makovicky et al., 2026). There is a prominent flange along the ventral surface of the distal two-thirds of metatarsal IV as in unenlagiines and to a lesser degree in other early-diverging dromaeosaurids and troodontids (Xu and Wang, 2000; Novas and Pol, 2005; Makovicky et al., 2026). Metatarsal V is a slender and curved bone, measuring 36% of metatarsal III length, more similar to dromaeosaurids than other pennaraptorans, which have significantly shorter metatarsal V (Xu and Wang, 2000).

Non-ungual pedal phalanges are in relatively long and slender, unlike the short and squat ones in typical cursorial theropods such as ornithomimids (Makovicky et al., 2004), parvicursorine alvarezsaurids (Perle et al., 1994), and oviraptorids (Makovicky et al., 2026). Non-ungual pedal phalanges display a decrease in length from proximal to distal direction in each digit: pedal phalanx II-2 is considerably shorter than II-1, measuring about 75% of the former length; pedal phalanx III-3 measures about 80% of the III-2 length; IV-4 is about 90% of IV-3 length. In most other early-diverging paravians, the penultimate pedal phalanges are elongated and are at least as long as the

preceding phalanges. Nearly all non-ungual pedal phalanges display dorsally displaced collateral ligamental pits. Pedal phalanx III-1 is the longest non-ungual pedal phalanx, and both pedal phalanges III-2 and -3 bear a proximoventral heel and the one of III-3 is elongated proximodistally and is more prominent. Pedal phalanx IV-1 is longer than II-1 (about 120% of the latter length) as in dromaeosaurids and early-diverging troodontids, and in anchiornithines and *Archaeopteryx*, pedal phalanx IV-1 is also elongated, but still shorter than II-1.

Pedal unguals are ventrally curved and bear a prominent flexor tubercle. The medial collateral groove is dorsally displaced in all pedal unguals. The ungual of pedal digit II is subequal in length to III-1. Its flexor tubercle is as deep dorsoventrally as the proximal articular facet of the ungual and displays a rounded ventral end in lateral view. A distinct groove, which is an extension of the collateral groove, defines the proximal border of the flexor tubercle in both sides and ventral surface. The flexor tubercle of pedal ungual III and IV is also slightly expanded transversely and extends slightly more ventrally than the preceding portion in lateral view.

3.3 Horny sheath and plumage

Horny sheath is preserved around the manual and pedal unguals (Figs. 9-12). In general, the majority of the horny sheath is preserved as impression, but the dorsal margin is preserved as three-dimensional structure. The horny sheath adds considerably the size and curvature of both manual and pedal claws: for example, there is 4.5-mm-long horny sheath distal to the 8.1-mm-long manual ungual II, and this horny sheath increases the curvature degree of the claw from about 120 degrees to more than 180 degrees along the dorsal margin; pedal claw II has an additional length of 4.5 mm besides the 7.5-mm-long ungual due to the horny sheath.

Feathers of various types and size cover the whole body (Figs. 13, 14), but the preservation makes it difficult to reveal detailed morphologies of individual feathers. Nevertheless, feathers covering the skull and mandible range from about 10 mm long to more than 35 mm long; the neck feathers are more than 35 mm in length; tail feathers attach to the whole length of body tail, with the anteriormost ones about 30 mm long, anterior and middle ones about 20 mm long, posterior ones about 40 mm long, and posteriormost ones about 200 mm long. The posteriormost feathers, which attach to about last five caudal vertebrae, are about 16 in number, and they seem to be rachis-dominant like the highly elongated tail feathers seen in some scansoriopterygids and many early-diverging avialans. These feathers are somewhat comparable to peacock tail feathers, which form a large fan-shaped surface.

Limb feathering is extensive, and as in microraptorines, anchiornithines, and the avialan *Sapeornis*, the feet are also extensively feathered. Remiges are in general long, and they display distinct curvature. As preserved, the longest primaries are located about the mid-length of metacarpus, a position between those of the longest primaries in *Microraptor* and anchiornithines. They are about 120 mm long (primary feather:humerus length ratio about 3.2 and primary feather:femur length ratio about 2.4), proportionally longer than those of the known non-avialan pennaraptorans (primary feather:humerus length ratio about 2.4, 2.4, and 1.2 in *Caihong*, *Microraptor* and *Caudipteryx*, respectively, and primary feather:femur length ratio about 2.0 in *Microraptor*). The secondaries are about 80 mm long, about 220% of the humeral length and about 160% of the femoral length, compared to about 120% and 105% in *Microraptor gui* holotype, respectively).

Large pennaceous feathers are also attached to the hindlimbs. The femoral feathers are at least 25 mm long, the longest tibial feathers are at least 35 mm in length, and the metatarsalian feathers are up to 60 mm long. It should be noted that long tibial feathers are present on either side of the bone. The longest metatarsal feathers are located more distally than in anchiornithines, closer in condition to microraptorines. They are intermediate in relative length between those of *Microraptor* and other known early-diverging pennaraptorans that bear large pedal feathers, for example, the longest metatarsalian feathers about 140% of the metatarsus length in *Changzhousaurus sinensis*, compared to about 320% in *Microraptor*, and about 120% of the femoral length in *Changzhousaurus sinensis*, compared to about 200% in *Microraptor*.

4 Discussion

The discovery of the pennaraptoran *Changzhousaurus sinensis* has implications in several aspects pertaining to pennaraptoran systematics, behaviors, and ecology, and particularly the transition to birds. A quantitative discussion of these aspects will be given elsewhere and here a qualitative discussion is presented. Additionally, I provide some comments on several methodological and conceptual issues related to pennaraptoran studies in the light of the new discovery.

4.1 Systematic position of *Changzhousaurus sinensis* and pennaraptoran systematics

Pennaraptora comprises several recently discovered small clades (e.g., Unenlagiinae, Microraptorinae, Scansoriopterygidae, Anchiornithinae, and Halszkaraptorinae) as well as four long-recognized major groups (i.e., Oviraptorosauria, Dromaeosauridae, Troodontidae, and Avialae). The monophyly of these groups is well supported, with most clades displaying a suite of unique features. Among the four major pennaraptoran groups, oviraptorosaurians are primarily herbivorous animals characterized by a highly specialized cranial skeleton (e.g., a tall, short skull with a long postorbital region and specialized joint between the upper and lower jaws). Dromaeosaurids are agile predators distinguished by some cranial features (e.g., a dorsally displaced maxillary fenestra, a quadrate with a triangular lateral process and a large quadrate foramen, a sinusoidal anterior border of the supratemporal fossa, a sharp sagittal crest, a distally twisted paroccipital process, and a dentary with subparallel concave dorsal and convex ventral edges) and a few postcranial features (e.g., epipophyses of cervical vertebrae placed distally on the postzygapophyses, a stiff tail composed of highly elongated chevrons and caudal prezygapophyses, a coracoid with a large fenestra or fossa on the distal ramus, and a proportionally long metatarsal V). Troodontids are long-legged animals diagnosed by several cranial features (e.g., an expanded and deep subotic recess, a prominent otosphenoidal crest, a triangular groove on the lateral surface of a triangular dentary, and a relatively large number of heterodont teeth) and some postcranial features (e.g., middle and posterior caudal vertebrae with reduced centra, posterior caudal vertebrae with a dorsal groove in the place of a neural spine, a transversely broad and flat pubic apron, an asymmetrical foot with a distinctly short, slender metatarsal II and a long, robust metatarsal IV). Avialae are primarily volant animals, possessing many flight-related features (e.g., a proportionally long humerus and forearm, and a localized scapula-coracoid articulation) and feet adapted for arboreality (e.g., a distally positioned, reversed, and enlarged hallux).

Among the recently discovered pennaraptoran clades, Scansoriopterygidae, Halszkaraptorinae, and Microraptorinae exhibit more distinct body plans, whereas Unenlagiinae and Anchiornithinae

are comparatively less distinct. The arboreal Scansoriopterygidae is characterized by an elongated lateral manual digit that considerably exceeds the lengths of the medial digits, a propubic pelvis with a pubis lacking a distal boot, and an elongate, dorsally curved, strap-like ischium without an obturator process. The semiaquatic Halszkaraptorinae is characterized by a dorsoventrally flattened premaxilla perforated by numerous neurovascular foramina, large and closely packed premaxillary teeth, an external naris posteriorly and dorsolaterally displaced, greatly elongated and specialized cervical vertebrae, anterior caudal vertebrae with horizontal zygapophyses and pronounced zygapophyseal laminae, and a mediolaterally compressed ulna with a sharp posterior margin. Microraptorinae is characterized by a heavily pitted antorbital fossa wall, extremely long middle caudal vertebrae, a large accessory coracoid fenestra, a large lateral tubercle on the pubic shaft, and a spatulate pubic foot. Unenlagiinae is diagnosed by an ilium with a posterodorsal concavity in lateral view, a femur with a proximally positioned scar-like fourth trochanter, a strongly ventrally arched pedal phalanx III-1, and penultimate pedal phalanges with extremely dorsally displaced collateral ligamental pits. Anchiornithinae is characterized by dorsal vertebrae with posteriorly expanded neural spines, a humerus with a very short deltopectoral crest, and anteriormost caudal vertebrae with rod-like transverse process.

However, the taxonomic composition and systematic positions of these clades have not yet reached a consensus. It is widely accepted that Oviraptorosauria is the sister group to Paraves (a clade including Dromaeosauridae, Troodontidae and Avialae); however, an avialan status for Oviraptorosauria has also been proposed and supported by some evidence (Maryanska et al., 2002; Lü, 2005; Zhang et al., 2008). Deinonychosauria, comprising Dromaeosauridae and Troodontidae, is generally accepted as a monophyletic group, yet alternative phylogenetic hypotheses—such as a clade formed by Dromaeosauridae and Avialae or by Troodontidae and Avialae (e.g., Forster et al. 1998; Gianechini et al. 2018) —have also been proposed and supported. Among the recently discovered small pennaraptoran clades, the dromaeosaurid affinity of Unenlagiinae, Microraptorinae, and Halszkaraptorinae, the oviraptorosaurian status of Scansoriopterygidae, and the avialan affinity of Anchiornithinae are more widely accepted in recent studies (Cau et al., 2017; Foth and Rauhut, 2017; Agnolín et al., 2019; Pei et al., 2020; Xu et al., 2023; Chen et al., 2025). Nevertheless, alternative phylogenetic hypotheses for these clades are also supported by some evidence. For example, Unenlagiinae and Microraptorinae have been considered early-diverging avialans (Agnolin and Novas, 2011; Agnolin and Novas, 2013); Scansoriopterygidae have been proposed as early-diverging paravians (Xu et al., 2015; Lefèvre et al., 2017) or early-diverging avialans (Zhang et al., 2008; Turner et al., 2012; Cau, 2018; Hartman et al., 2019); and Anchiornithinae have been classified as early-diverging avialans (Balanoff et al., 2009; Wang et al., 2025), early-diverging troodontids (Hu et al., 2009; Turner et al., 2012; Godefroit et al., 2013), early-diverging deinonychosaurians (Xu et al., 2011; Godefroit et al., 2013), or early-diverging paravians (Lefèvre et al., 2017).

Besides the unresolved systematic affinities of these clades, the phylogenetic placement of many pennaraptoran species also remains ambiguous. For instance, the dromaeosaurids *Tianyuraptor*, *Zhengyuanlong*, *Shanag* and *Bambiraptor* have been assigned to Microraptorinae in some studies yet within Eudromaeosauria in others (Agnolín et al., 2019; Makovicky et al., 2026). Similarly, the unenlagiinine *Rahonavis* and the early-diverging avialan *Zhongornis* have alternatively been interpreted as an early-diverging avialan and a scansoriopterygid, respectively (Agnolín et al., 2019; Makovicky et al., 2026). Even greater controversy surrounds the taxonomic

composition of Anchiornithinae: it is uncertain whether the enigmatic *Yixianosaurus longimanus* (Xu and Wang, 2003; Xu et al., 2013; Cau et al., 2017) and the troodontid *Liaoningvenator curriei* (Shen et al., 2017) from the Early Cretaceous of Liaoning, China, and the *Pedopenna daohugouensis* from the Middle-Late Jurassic of Inner Mongolia, China (Xu and Zhang, 2005; Foth and Rauhut, 2017) belong to this clade. Debates intensify further regarding the placement of the iconic *Archaeopteryx* (Xu et al., 2011) and *Ostromia crassipes* (Foth and Rauhut, 2017) from the Late Jurassic of Bavaria, Germany, whose membership within Anchiornithinae is also contested.

Unstable phylogenetic relationships and systematics among pennaraptorans arise from multiple factors. These include reduced morphological gaps between pennaraptoran clades following recent discoveries, which blur their overall body-plan distinctions; the complex combination of morphological features in pennaraptoran taxa, generating conflicting phylogenetic signals; extensive missing data stemming from taphonomic preservation (e.g., incomplete skeletons or complete but heavily compressed specimens) and insufficient detailed analyses of many fossils (for example, many oviraptorosaurian features derive from palatal structures, which are difficult to observe in compressed cranial skeletons of most Mesozoic Chinese pennaraptorans, especially early avialans); and inconsistent character and taxon sampling across phylogenetic studies.

The conflicting phylogenetic signals warrant particular attention. For example, several diagnostic features of the aforementioned clades are also seen in some other pennaraptoran taxa. A relatively tall skull and robust mandible occur variably in scansoriopterygids and some early-diverging avialans; flight-related features and inferred aerial behaviors characteristic of early avialans are variably expressed in certain scansoriopterygids, unenlagiines, microraptorines, and anchiornithines; some microraptorine features exhibit broader phylogenetic distribution (e.g., a spatulate pubic foot is present in some early-diverging troodontids such as *Sinovenator*); and nearly all diagnostic features of Anchiornithinae are variably developed among troodontids, avialans, and some other pennaraptoran taxa. Furthermore, although the monophyly of Deinonychosauria is supported by several derived features across the skeleton (e.g., a laterally exposed splenial, highly modified pedal digit II, a prominent ventral flange on metatarsal IV, and an elongated pedal phalanx IV-1), alternative phylogenetic hypotheses are supported by some other morphological evidence. For example, a Troodontidae-Avialae clade is supported by braincase and reproductive features and a Dromaeosauridae-Avialae clade is supported by some features from appendicular skeleton. The discovery of *Changzhousaurus sinensis* further exemplifies this pervasive phylogenetic ambiguity.

Changzhousaurus sinensis is clearly a pennaraptoran dinosaur based on numerous derived similarities shared with other early-diverging pennaraptorans. These features include external naris large and posteriorly extending to the level of antorbital fossa, the anterior-most caudal vertebrae anteroposteriorly shortened, the middle caudal vertebrae significantly elongated, the anteriorly located caudal transitional point, scapula with acromion process laterally everted, strongly inflected coracoid, scapulocoracoid L-shape in lateral view and with a laterally facing glenoid fossa, an ilium with a lobate, long preacetabular process (about 60% the iliac length), and a caudoventrally directed pubis with a reduced anterior pubic boot. It should be noted that some of these features have been considered to be paravian features by some studies (Makovicky et al., 2026), but they are also known in some oviraptorosaurian dinosaurs including scansoriopterygids and thus are more likely to be pennaraptoran features.

Changzhousaurus sinensis is assignable to Paraves based on numerous derived features that it shares with other paravians. These features include a short and subtriangular skull in lateral view,

the sacral zygapophyses fused to form a platform lateral to the fused neural spines, a wide pubic peduncle about 30% of the iliac length, a partial supraacetabular crest covering only anterior half of the iliac acetabular margin, strap-like ischium short (about 40% the pubic length) and with a posteroproximal process and a posterodistal process.

Changzhousaurus sinensis displays the following derived features that are present in at least some dromaeosaurids and troodontids but absent in most other pennaraptorans. These features include T-shaped lacrimal with a prominent lateral flange over orbital anterodorsal corner, heterodont dentary tooth row with anterior dentary teeth slender, closely packed and posterior dentary teeth stout and relatively widely distributed, pubis with spatulate distal end in lateral view, a robust metatarsal II, a metatarsal III with a transversely compressed proximal portion and a ginglymoid distal articular surface, a metatarsal IV with a prominent ventral flange, a specialized pedal digit II with distally expanded pedal phalanx II-1 and a large II-3 with prominent flexor tubercle, and a pedal phalanx IV-1 longer than II-1.

Among deinonychosaurians, *Changzhousaurus sinensis* displays a combination of both dromaeosaurid and troodontid features. For example, it possesses some derived features seen in at least some troodontids but absent in most other pennaraptorans including dromaeosaurids, including maxillary anterior ramus with a concave dorsal margin for receiving premaxillary maxillary process and contributing to posterior half of external naris ventral border, antorbital fossa anteriorly and ventrally poorly defined (at least in *Mei long* holotype), interfenestral bar flushing with snout lateral surface (at least in *Bynosaurus* and *Mei long* holotype), small rounded maxillary fenestra (probably in *Mei long* holotype), asymmetrical foot with distinctly narrower and shorter metatarsal II and longer and more robust metatarsal IV. Meanwhile, *Changzhousaurus sinensis* displays some derived features seen in at least some dromaeosaurids but absent in most pennaraptorans including troodontids. These features include dentary with nearly parallel concave dorsal margin and convex ventral margin in lateral view, a sharp sagittal crest along the midline of the fused parietal, coracoid with a large fossa on distal ramus posterior surface, an ilium with ventrally extended postacetabular process in lateral view, and a proportionally long metatarsal V (Makovicky et al., 2026). The discovery of *Changzhousaurus sinensis* thus provides additional evidence supporting deinonychosaurian monophyly.

However, *Changzhousaurus sinensis* also exhibits some features with alternative phylogenetic signals. For example, it displays some derived features suggesting a close relationship with both troodontids and anchiornithines. These features include postorbital with a long slender and anteriorly curved jugal process, quadrate strongly curved posteriorly, dentary lateral surface bearing a posteriorly broadened longitudinal groove, maxillary tooth row extending posteriorly about preorbital bar level (at least in *Mei long* holotype), and radius only slightly thinner than ulna. Meanwhile, it displays the following derived features shared with Troodontidae, Anchiornithinae and *Archaeopteryx,* including cervical vertebrae transversely much wider than long, anterior-most caudal vertebrae with slender transverse processes, and middle and posterior caudal vertebrae with short anteriorly-oriented prezygapophyses. Particularly noteworthy is that *Changzhousaurus sinensis* shares with the anchiornithine *Xiaotingia* a few derived features. For example, both taxa have an anteriorly bowed radius (also present in *Buitreraptor*), a large and wide iliac pubic peduncle (also in *Rahonavis*), a slender, straight, strap-like ischial shaft with thickened anterior margin (also in some microraptorines), and ischial pubic peduncle long and distally tapered and ischial iliac peduncle short and robust and aligned with the ischial shaft. *Changzhousaurus sinensis* has a long

and robust metacarpal IV as in *Xiaotingia*, Enantiornithine, Scansoriopterygidae, *Mei long*, Halszkaraptorinae, and particularly it is similar to the latter three taxa in having a manual digit IV subequal to or even longer than digit III, which is unusual among theropod dinosaurs. Finally, *Changzhousaurus sinensis* might possess several derived features seen in at least some avialans but not in most non-avialan pennaraptorans: an incipient procoracoid process, a large, V-shaped ulnare, a proximodistally deep 'semilunate' carpal, and an ischium with distally oriented rectangular obturator process.

In summary, *Changzhousaurus sinensis* is most likely an early-diverging deinonychosaurian, and its discovery provides additional evidence for the monophyly of Deinonychosauria. Meanwhile, alternative systematic positions such as anchiornithine or avialan status are also not impossible, and its discovery even provides some evidence for a clade including dromaeosaurids, troodontids, anchiornithines, *Archaeopteryx*, and euornithine birds (see below for further comments). Nevertheless, the discovery of *Changzhousaurus sinensis* further highlights the complex character distribution among early-diverging pennaraptorans and brings more difficulties in recovering a robust pennaraptoran phylogeny.

Several approaches can be adopted to resolve a robust pennaraptoran phylogeny. The first is to extract additional phylogenetic signals from existing pennaraptoran fossil material. Fine yet stable morphological variations can be formulated as new characters and incorporated into datasets for pennaraptoran phylogenetic analyses. For instance, the monophyly of Deinonychosauria is conventionally supported by the specialized second pedal digit, but notable morphological differences in this structure between troodontids and dromaeosaurids can be formulated as novel characters to further improve phylogenetic resolution. A second way is to expand taxon sampling to resolve long ghost lineages. Current mainstream hypotheses of pennaraptoran phylogeny recognize at least two prolonged ghost lineages within Dromaeosauridae: the unenlagiine and halszkaraptorine clades. Increased sampling of taxa from these lineages will help stabilize the phylogenetic positions of these clades within Pennaraptora.

Expanding datasets via more characters and denser taxon sampling is a standard practice in modern phylogenetics. However, recent phylogenetic studies have shown that this approach is not always effective (Lovegrove et al., 2024). In some cases, larger datasets have weakened or even falsified long-standing phylogenetic hypotheses. While the impact of *Changzhousaurus sinensis* on quantitative phylogenetic reconstruction of Pennaraptora remains unclear, its unique combination of morphological characters likely reduces nodal support for several established pennaraptoran clades. Specifically, *Changzhousaurus sinensis* possesses diagnostic features previously used to define Unenlagiinae and Anchiornithinae; its inclusion in quantitative analyses tends to lower support values for both clades.

Widespread homoplasy among early-diverging pennaraptorans arises from multiple causal factors. First, distantly related pennaraptoran taxa often share similar ecologies and behaviours, driving convergent evolution of corresponding morphological characters. Second, homoplasy may stem from incomplete lineage sorting or rapid cladogenesis during lineage diversification. A third factor, which has received limited attention to date, is hybrid speciation — a phenomenon common among crown birds. All these issues call for methodological innovations, for example, integrating phylogenetic networks alongside traditional tree-based analyses, and new analytical frameworks that recognise topological polytomies as biological signals, rather than treating them merely as analytical uncertainty.

While expanded data collection and methodological advances are still essential for reconstructing a robust pennaraptoran phylogeny via quantitative approaches, it is recommended to conduct qualitative character assessment prior to formal phylogenetic analyses. Such assessments can guide the construction of more reliable datasets and at least help to find potential issues pertaining to phylogenetic reconstruction. This qualitative evaluation can be approached from multiple perspectives.

First, we should revisit whether distinct morphological characters are required for phylogenetic inference across different taxonomic ranks. In molecular systematics, gene selection is a core consideration: deep-level phylogenies rely on conserved genes, whereas analyses of shallow divergences use rapidly evolving genes (Soltis and Soltis, 1998; Rick et al., 2024). In contrast, few studies have discussed whether morphological characters can be partitioned in a comparable way, or whether different character sets are needed for analyses at varying taxonomic levels.

Second, the pervasive occurrence of convergence and character reversal necessitates careful evaluation of their impacts on phylogenetic reconstruction. Characters associated with flight show complex distributions among early-diverging pennaraptorans, likely resulting from either multiple independent origins of aerial locomotion or repeated secondary loss of flight capability during early pennaraptoran evolution. Accordingly, analysing morphological features unrelated to flight may yield more reliable phylogenetic signals. Cranial morphology notably separates early pennaraptorans into two distinct groups. The first clade comprises Oviraptorosauria, Scansoriopterygidae, and non-euornithine avialans excluding *Archaeopteryx*, characterised by robust crania and reduced dentition. The second group includes Dromaeosauridae (including Unenlagiinae, Microraptorinae, Halszkaraptorinae), Troodontidae, Anchiornithinae, *Archaeopteryx* and Euornithes, distinguished by lightweight, more kinetic crania and well-developed dentition. Further testing is required to verify whether this cranial dichotomy reflects true phylogenetic relationships. Congruent patterns in postcranial characters unrelated to flight would provide strong corroboration for this grouping. Overall, qualitative character evaluation, paired with new quantitative methods that account for the above issues, will greatly facilitate the reconstruction of a well-supported pennaraptoran phylogeny.

4.2 Locomotion and habitat ecology of early-diverging pennaraptorans

ly on analogue-based comparisons. This approach performs reliably when extinct and extant Non-avialan pennaraptoran dinosaurs have long been considered as terrestrial cursors, but some recent studies suggest that they may be diverse in habitat ecology and locomotion styles (Xu et al., 2003; Xu et al., 2015; Cau et al., 2017; Lee et al., 2022), with some being tree-dwelling flyers (e.g., *Yi, Anchiornis* and *Microraptor*) and other being aquatic animals (e.g., *Halszkaraptor* and *Natovenator*) (Xu et al., 2003; Xu et al., 2015; Lee et al., 2022). These studies, despite presenting different views of pennaraptoran habitat ecology and locomotion, are all based on the same approach, i.e., *uniformitarian* approach, which means that ancient life follow the same rules of physics, chemistry and biology derived from living organisms. More specifically, these studies applied two widely used methods (i.e., ecomorphological inference and biomechanical analysis) developed under the uniformitarian framework, and both methods are heavily dependent on “rules” derived from living animals.

Multiple factors account for the ongoing debates over habitat preference and locomotor ecology among pennaraptorans. First, disparate datasets and analytical methods across studies often

yield divergent functional rules extrapolated from extant organisms. For instance, limb proportions indicate *Anchiornis* was a cursorial animal, yet its extensive leg feathers suggest poor running performance (Hu et al., 2009). Similarly, limb bone geometry implies *Archaeopteryx* was an active flyer (Voeten et al., 2018), while evidence from shoulder girdle morphology and feather rachises points to limited flight capacity or even a complete lack of aerodynamic function (Senter, 2006; Nudds and Dyke, 2010).

Even a single morphological character can lead to contradictory interpretations of target behaviours. A classic example involves flight feather asymmetry: this character has been interpreted as evidence for flight capability in *Archaeopteryx* (Feduccia and Tordoff, 1979), yet other studies have cited the same feature to challenge this hypothesis (Shipman, 1998). Characters including a reversed hallux, elongated penultimate pedal phalanges and curved pedal claws are widely regarded as indicators of arboreality in early-diverging pennaraptorans including *Archaeopteryx* (Feduccia, 1999). Nevertheless, several studies have rejected this conclusion using comparable comparative datasets (Glen and Bennett, 2007).

Fig. 13 Plumage of *Changzhousaurus sinensis* holotype (LDNHMF 2026A)

A. feathers associated with mandible and neck; B. feathers associated with right forearm and manus; C. feathers associated with right ulna; D. feathers associated with medial side of right tibia; E. feathers associated with lateral side of right tibia. Scale bars=1 cm

These cases demonstrate that establishing reliable functional rules based solely on extant taxa can be problematic, though building comprehensive comparative datasets from modern organisms remains essential. One solution is to construct more rigorous comparative datasets, and selecting suitable extant analogues is equally important in this regard. For assessing arboreality in early-diverging pennaraptorans, for example, functional frameworks derived from flightless birds or non-avian flightless tetrapods are more suitable than those from volant birds, which possess two highly specialised locomotor systems.

A second consideration for *uniformitarian* approach is the substantial morphological disparity

between stem and crown members of a clade (e.g., stem and crown birds). Such differences greatly complicate, and may even mislead, ecomorphological and biomechanical inferences based on extant analogues. Notably, scansoriopterygids possess membranous rather than feathered wings, meaning modern birds are not perfect analogues for reconstructing their flight behaviours. Two solutions are available to address this issue. One is to adopt alternative extant models; bats, for example, can serve as analogues for studying wing function in scansoriopterygids if membranous and feathered wings are drastically different regarding to aerodynamic performance. The other is to infer behaviours of extinct taxa using well-documented characters of closely related extinct species. Scansoriopterygids were likely arboreal, and their ecological characters can provide valuable comparative data for evaluating arboreality in other early-diverging pennaraptorans.

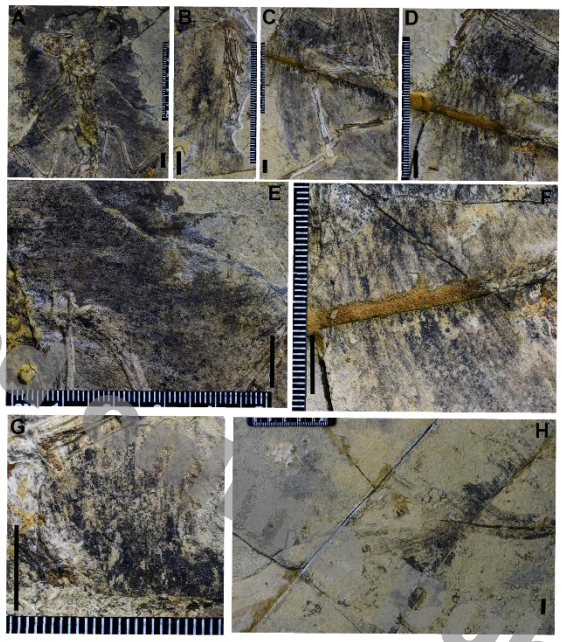

Fig. 14 Plumage of *Changzhousaurus sinensis* holotype (LDNHMF 2026B)

A. feathers associated with skull and neck; B. feathers associated with left forearm and manus; C. feathers associated with right forelimb and hindlimb; D. feathers associated with right forearm and manus; E. feathers associated with neck and left humerus; F. primaries associated with right manus; G. feathers associated with right femur and anteriormost caudal vertebrae; H. highly elongated tail feathers associated with the posterior end of the bony tail. Scale bars=1 cm

Third, ancient physical environments differed drastically from modern conditions, and such disparities strongly influenced animal behaviours. Previous research has confirmed that aerial behaviours were far more prevalent when atmospheric density was elevated (Dudley, 1998). Accordingly, biomechanical models parameterised using modern environmental conditions tend to underestimate flight performance in these ancient ecosystems. It is therefore necessary to conduct tests under more realistic palaeoenvironmental settings. For example, modelling flapping flight of early-diverging pennaraptorans under high air density is preferable to fixed-wing simulations under modern conditions, despite greater technical and methodological challenges.

In summary, current ecomorphological and biomechanical analyses predominantly retaxa share similar morphologies, fossil characters are well-resolved, and their habitats are comparable. However, its efficacy declines when these prerequisites are unmet, under which circumstances an

evolutionary framework becomes a viable alternative.

Novel functions or behaviours can evolve without major morphological changes, a pattern best illustrated by exaptation — an evolutionary process where a pre-existing character is co-opted for a new role. In most cases, new behaviours emerge prior to the evolution of corresponding phenotypic modifications. Subsequent morphol13ogical adaptations further refine these newly acquired functions, until highly specialised structures eventually evolve for the derived behaviour. As such, robust evolutionary trends inferred from multiple lines of evidence can support the presence of a novel function, even when analogue-based analyses fail to do so.

The locomotor behaviours of early-diverging pennaraptorans, including aerial locomotion and arboreality, exemplify the utility of this evolutionary approach. Many early-diverging pennaraptorans — such as scansoriopterygids, unenlagiinines, microraptorines, anchiornithines and *Archaeopteryx* — are hypothesised to have possessed flight abilities of varying degrees, though this view remains contested. Debates persist regarding the functional roles of leg feathers and membranous wings in aerial locomotion, as well as flight modes (flapping versus gliding) in these taxa (Padian, 2003; Foth et al., 2014; Kiat and O'Connor, 2024)

An evolutionary framework places behavioural interpretations within a phylogenetic context. A suite of flight-related characters evolved at the base of Pennaraptora, including laterally mobile elongated forelimbs, flight-associated plumage, complex brains adapted to dynamic environments, and elevated metabolic rates. Linking these phenotypic innovations to aerial behaviours represents the most parsimonious interpretation, even if certain individual characters contradict flight capacity when evaluated against extant analogues. For example, flight feather morphology in *Anchiornis* seems inconsistent with active flight based on modern bird standards, yet its overall phenotypic suite supports flight capability as a paravian. From an evolutionary perspective, the multi-layered wings formed by its slender, symmetrical flight feathers could function equivalently to the single-layered wings of large, asymmetrical flight feathers in modern flyers (Longrich et al., 2012; Xu, 2012). Similarly, although some early-diverging pennaraptorans have been interpreted as gliders, an evolutionary approach favours flapping flight. This applies even to bat-winged scansoriopterygids, as their osteology closely resembles that of early flapping birds, their descendants within maniraptoran phylogeny.

The evolutionary approach also clarifies the debate between cursoriality and arboreality in early-diverging pennaraptorans. Non-avialan theropods are universally recognised as cursorial, and this lifestyle represents the ancestral behavioural state for the clade. Corresponding to this ecology, they typically have short, robust pedal phalanges and flat claws. In contrast, early-diverging pennaraptorans including *Microraptor*, *Anchiornis* and *Archaeopteryx* exhibit derived pedal features: elongated penultimate phalanges, curved claws, and in some cases a fully reversed hallux. These characters signal an adaptive shift toward arboreality. An evolutionary perspective thus supports arboreal habits in these taxa, even though pedal morphospace analyses often do not group them with extant arboreal birds.

It is worth noting that *Changzhousaurus sinensis* represents an especially problematic taxon for reconstructing ancestral habitat ecology and locomotor modes. This species possesses the largest known feathered wings among non-avialan pennaraptorans, and such wing morphology, coupled with key osteological modifications (e.g., laterally flappable forelimbs), strongly supports the presence of flight capability. However, its flight feathers are slender and lack the robust rachises, seemingly indicating limited or absent flight capacity. In terms of pedal morphology,

Changzhousaurus sinensis exhibits slender, elongated pedal phalanges typical of other early-diverging pennaraptorans, yet it bears a smaller, more proximally positioned hallux and proportionally shorter penultimate pedal phalanges, pointing to a distinct ecological adaptation relative to its close relatives.

Given these conflicting morphological signals regarding the habitat preferences and aerial behaviours of *Changzhousaurus sinensis*, an evolutionary framework is essential for robust behavioural reconstruction. From an evolutionary perspective, the presence of flight capability is well supported, whereas its unusual pedal morphology likely represents an evolutionary reversal. Specifically, *Changzhousaurus sinensis* is derived from arboreal pennaraptoran ancestors characterised by proportionally elongated penultimate phalanges and larger, more distally positioned halluces, and it secondarily modified its pedal apparatus for a more terrestrial environment.

Comprehensive and rigorous analyses are still required to fully resolve the locomotor and ecological characters of *Changzhousaurus sinensis*. A recent study that quantified evolutionary flight loss rates across early-diverging pennaraptorans and identified secondarily flightless taxa (Kiat and O'Connor, 2024) provides an excellent methodological template for future behavioural investigations of this enigmatic taxon.

4.3 Pennaceous feather evolution and definitions of feathers and birds

Changzhousaurus sinensis exhibits full-body plumage comprising diverse feather types and sizes, with well-developed pennaceous feathers distributed across the forelimbs, hindlimbs, and tail. Nevertheless, its plumage morphology differs substantially from that of other early-diverging pennaraptorans in several key aspects. First, the wing feathers form a unique feathered wing apparatus distinct in both shape and size from those of other early-diverging pennaraptorans (Foth and Rauhut, 2020). *Changzhousaurus sinensis* possesses the proportionally largest feathered wings among all known non-avialan pennaraptorans, and its longest primary feathers attach at a more proximal position compared with those of microraptorines and most early-diverging avialans. Second, the hindlimb plumage of *Changzhousaurus sinensis* also exhibits unique traits. Its tibial feathers are proportionally longer than those of other early-diverging pennaraptorans, while its metatarsal feathers are elongated and orient somewhat proximally, in contrast to the nearly perpendicular metatarsal plumage observed in anchiornithines and *Sapeornis*. Finally, the tail plumage of *Changzhousaurus sinensis* combines morphological features observed in multiple pennaraptoran clades while also presenting unique derived character states. On one hand, its feathered tail exhibits a fan-like configuration reminiscent of *Jeholornis* and, to a lesser extent, some oviraptorosaurs, with large pennaceous feathers anchored to the posterior caudal vertebrae. In comparison, *Archaeopteryx*, anchiornithines (e.g., *Anchiornis*, *Caihong*), and troodontids (e.g., *Jiangnianhualong*, *Jinfengopteryx*) possess frond-like tails, in which nearly uniformly sized large pennaceous feathers span the entire caudal length. Microraptorines represent an intermediate condition, with large pennaceous feathers restricted to the posterior half of the bony tail and distal feathers exhibiting greater elongation. On the other hand, *Changzhousaurus sinensis* converges with some scansoriopterygids, confuciusornithids, and enantiornithines in possessing highly elongated rachis-dominant tail feathers. Notably, however, the number of these elongated tail feathers in *Changzhousaurus sinensis* (approximately 16) far exceeds that recorded in other taxa (typically two to four). Although some microraptorines such as *Changyuraptor* also bear elongated posterior tail

feathers, their elongation is less pronounced, and they retain typical rectricial morphology.

The discovery of *Changzhousaurus sinensis* highlights the remarkable morphological diversity and complexity of limb and tail plumage among early-diverging pennaraptorans. Elongated tail feathers and extensive hindlimb feathers have been documented across multiple early-diverging pennaraptoran lineages: highly elongated tail feathers characterize scansoriopterygids and early avialans, whereas prominent pedal feathers are typical of microraptorines, anchiornithines, and *Sapeornis*. These plumage features are hypothesized to function in flight, visual communication, or both in early pennaraptorans. *Changzhousaurus sinensis* represents the first documented early-diverging pennaraptoran to concurrently possess both highly elongated tail feathers and large pedal feathers. Although this study does not aim to systematically investigate the functional significance of these plumage features, a purely communicative function for both pedal and tail feathers appears biologically implausible. Instead, these feathers likely contributed to aerial locomotion, consistent with the specialized osteological modifications and putative sensory adaptations for flight documented in other early-diverging pennaraptorans. Furthermore, *Changzhousaurus sinensis* provides critical insights into the evolution of feathered wing architecture. Bony forelimb length has long been widely adopted as a proxy for wing size and aerial locomotor capacity in fossil taxa. Despite its proportionally short bony forelimbs, *Changzhousaurus sinensis* bears the largest proportional feathered wings among non-avialan pennaraptorans, demonstrating significant morphological decoupling between skeletal forelimb dimensions and soft-tissue wing size. This finding indicates that a proportionally short bony forelimb cannot be reliably interpreted as conclusive evidence for small wing size or absent flight capability in early-diverging pennaraptorans.

Furthermore, the discovery of *Changzhousaurus sinensis* raises fundamental implications for the methodological practice of fossil feather research and even the conceptual definition of feathers themselves. Over the past three decades, abundant well-preserved feathered dinosaur fossils from China and other regions have firmly established that diverse feather morphologies evolved long before the origin of Avialae (Foth and Rauhut, 2020; Pittman and Xu, 2020). Fossil evidence further indicates that simple monofilamentous feathers represent the ancestral feather morphotype, with complex vaned feathers evolving later within feather evolutionary history. These findings also reveal that early fossil plumage differs from modern avian feathers in morphology, spatial distribution, and developmental characteristics. Despite substantial advances in understanding the origin and early diversification of feathers, numerous conceptual and methodological challenges remain unresolved.

Changzhousaurus sinensis exemplifies several issues in fossil feather research. First, fine morphological details are poorly preserved in the *Changzhousaurus sinensis* holotype. Although pennaceous feathers are extensively preserved across the entire skeleton—particularly along the limb bones and caudal series—diagnostic microstructures for pennaceous feathers cannot be confirmed. Critical features including barbules are not observable in the fossil plumage, and precise measurements of feather and vane dimensions are unobtainable. Nevertheless, these structures are assigned to pennaceous feathers based on their overall morphological similarity to confirmed pennaceous feathers in other early-diverging pennaraptoran fossils and modern avian counterparts. This dilemma is pervasive in fossil feather studies: many fossil feathers are attributed to specific morphotypes based on gross morphology, even when key diagnostic microscopic features are not preserved. This taxonomic uncertainty complicates accurate interpretation of early feather evolution.

Preservation biases affect not only individual feather morphology but also reconstructed

plumage distribution patterns. *Changzhousaurus sinensis* is a four-winged pennaraptoran, a condition hypothesized to have played a pivotal role in pennaraptoran evolution and the origin of dinosaur flight (Xu et al., 2003; Zheng et al., 2013; Xu et al., 2014a; Xu and Barrett, 2025). However, the locomotor function and phylogenetic distribution of extensive pedal feathering remain contentious. For instance, several anchiornithine and microraptorine specimens have been interpreted as lacking elaborate hindlimb plumage (Godefroit et al., 2013; Foth et al., 2014), yet taphonomic loss cannot be excluded as an alternative explanation. Confirming the true absence of soft-tissue structures in fossil specimens is methodologically challenging, highlighting a core limitation of paleoplumage research: taphonomic and fossilization processes can substantially distort original biological data (Xu and Barrett, 2025). Although experimental taphonomic studies have attempted to address this issue, distinguishing genuine biological traits from taphonomic artifacts remains a critical challenge for objective fossil feather characterization.

Modern avian feathers are defined by a unique suite of biochemical, cellular, developmental, and morphological features that accumulated gradually during archosaur evolution (Chuong et al., 2003). Current paleontological practice generally interprets fossil feathers as transitional forms toward modern feather morphologies. However, inconsistent classification practices persist: many fossil feathers are assigned to modern feather categories despite exhibiting distinct, potentially divergent morphological characteristics. For example, some fossil pennaceous feathers (e.g., those of *Anchiornis*) are inferred to possess open vanes (Saitta et al., 2017), yet remain classified as pennaceous. This inconsistency raises a fundamental conceptual question: how should fossil integumentary structures with morphology, distribution, and developmental patterns divergent from modern feathers be categorized? This ambiguity applies to multiple controversial structures, including the putative flight feathers of early-diverging pennaraptorans and monofilamentous integumentary structures in non-avialan dinosaurs and pterosaurs. Distinct terminology has been proposed for pterosaur monofilaments (Kellner et al., 2010), though some studies identified them as primitive feathers (Yang et al., 2019). Additionally, most diagnostic developmental and cellular features of modern feathers are not fossilizable, creating persistent uncertainty regarding the morphological disparity between modern and fossil feathers. These ambiguities fuel ongoing debates concerning the timing of feather origins (Barrett et al., 2015; Benton et al., 2019) and the functional and morphological disparity between flight feathers in early-diverging pennaraptorans and modern birds (Feo et al., 2015).

A potential solution to this conceptual confusion can be drawn from PhyloCode nomenclatural practices. The PhyloCode framework systematically distinguishes crown and stem taxa to accommodate fundamental disparities in data availability and dramatic differences between extant and extinct organisms. Similarly, fossil integumentary structures differ from modern feathers in both biological characteristics and observable morphological data. I therefore propose adopting a stem–crown distinction for feather terminology. General terms such as “feathers” and “pennaceous feathers” may be retained for practical descriptive purposes, but fossil integumentary structures should be formally designated as stem-group feathers or stem-group pennaceous feathers to explicitly differentiate them from derived crown-group avian feathers, consistent with phylogenetic nomenclature principles.

A further understudied issue involves the disconnect between technical taxonomic terminology and vernacular public terminology, a critical consideration given the broader societal impact of paleontological discoveries. Taxonomic revisions over recent decades have reshaped fundamental

biological definitions and gradually permeated popular culture and public understanding. For example, phylogenetic definitions under the PhyloCode formally include modern birds within Dinosauria, fundamentally altering conventional public perceptions of dinosaurs. The evolutionary origination of avian traits (e.g., feathers, flight) deep within maniraptoran phylogeny further complicates the definition of "birds". The technical clade name Aves was originally defined based on diagnostic morphological traits of extant birds, aligning closely with the traditional vernacular definition of birds as feathered, flying animals. Many extinct taxa, including *Archaeopteryx*, have been assigned to Aves due to their possession of key avian traits such as feathers and flight, despite lacking other crown avian features such as a keratinous beak.

The taxonomic expansion of Aves remains controversial among researchers, with some studies advocating for retention of the original crown-restricted definition. The clade name Avialae was subsequently established to encompass both crown birds and feathered, flight-capable stem avian relatives such as *Archaeopteryx*. While the debate over Aves delimitation lies beyond the scope of this study, the vernacular definition of "birds" has broadly expanded in public discourse to encompass all feathered, flight-capable dinosaurs, effectively aligning popular usage with the technical definition of Avialae. Multiple non-avialan pennaraptorans, including oviraptorosaurs, troodontids, and dromaeosaurids, are now known to possess complex pennaceous feathers and even flight capacity. By traditional historical standards applied to *Archaeopteryx* (Xu, 2024), these feathered non-avialan dinosaurs would qualify as "birds". This paradigm shift calls for renewed communication with the public to update popular understanding of avian origins and dinosaur diversity, acknowledging that the evolutionary family of feathered, bird-like dinosaurs is far more extensive than previously recognized.

Acknowledgements The author thank Mr. LU Jianhua for providing the access to studying the specimen, China Dinosaur Land Culture & Tourism Group Co. Ltd. for promoting popular science of dinosaur paleontology and supporting this study, ZANG Hailong for the figures, DING Xiaoqing for fossil preparation, XIANG Lishi and ZANG Hailong for the casts, and HU Dongyu and ZHAO Qi for comments and suggestions. This study was supported by the National Key R&D Program of China (2025YFF0811700) and the National Natural Science Foundation of China (grant no. 42288201)

中国北方早白垩世一新的长羽毛恐龙彰显廓羽盗龙类早期演化复杂性及对若干相关概念和方法的评论

徐 星

(中国科学院古脊椎动物与古人类研究所 北京 100044)

摘要：近期的早期分异廓羽盗龙类化石发现推进了鸟类起源研究，尤其揭示了像羽毛和飞行能力这样的鸟类定义性特征的演化。基于产自中国辽宁西部下白垩统九佛堂组的一件化石，我在

本文报道一新的鄑羽盗龙类。尽管这一新物种具有不同鄑羽盗龙支系的衍征，它很可能属于早期分异的恐爪龙类。最重要的是，这一新物种展现了特别异常的羽毛特征：它代表首个同时具有大型足羽和极度加长尾羽的鄑羽盗龙类；长尾羽数量明显多于其他早期分异的鄑羽盗龙类，某种程度和孔雀尾羽表面相似；它的翼羽形成了非鸟鄑羽盗龙类中相对最大的羽翼—尽管其骨质前肢较短—这指示前肢骨骼长度和羽翼面积不相关。这一发现彰显了鄑羽盗龙类早期演化的复杂性，并引发了鄑羽盗龙类研究当中的存在的几个概念性和方法性问题，包括如何重建一个稳健的鄑羽盗龙类系统发育、如何推断早期鄑羽盗龙类的飞行行为和栖息地生态以及如何定义羽毛和鸟类。

关键词：辽宁建昌；早白垩世；九佛堂组；鄑羽盗龙类；羽毛；系统发育；形态；栖息地生态和飞行行为

References

Agnolin F L, Novas F E, 2011. Unenlagiid theropods: are they members of the Dromaeosauridae (Theropoda, Maniraptora)? An Acad Bras Cienc, 83(1): 117–162

Agnolin F L, Novas F E (2013). Review of the phylogenetic relationships of the theropods Unenlagiidae, Microraptoria, Anchiornis and Scansoriopterygidae. Dordrecht, Springer.

Agnolín F L, Motta M J, Egli F B et al., 2019. Paravian phylogeny and the dinosaur-bird transition: an overview. Frontiers in Earth Science 6: 252

Alexander D E, Gong E, Martin L D et al., 2010. Model tests of gliding with different hindwing configurations in the four-winged dromaeosaurid Microraptor gui. Proceedings of the National Academy of Sciences of the United States of America, 107(7): 2972–2976

Balanoff A M, Xu X, Kobayashi Y et al., 2009. Cranial Osteology of the theropod dinosaur Incisivosaurus gauthieri (Theropoda: Oviraptorosauria). Am Mus Novit, 3651: 1–36

Barrett P M, Evans D C, Campione N E, 2015. Evolution of dinosaur epidermal structures. Biology Letters online preprint, 11(6):

Benton M J, Dhouailly D, Jiang B et al., 2019. The early origin of feathers. Trends in ecology & evolution, 34(9): 856–869

Bonaparte J F, 1999. Tetrapod faunas from South America and India: A paleobiogeographic interpretation. Proceedings of the Indian National Science Academy, 65: 427–437

Brusatte S L (2011). Dinosaur Paleobiology. Chichester, Wiley-Blackwell.

Brusatte S L, O'Connor J K, Jarvis E D, 2015. The origin and diversification of birds. Current Biology, 25(19): R888–R898

Cau A, Beyrand V, Voeten D F A E et al., 2017. Synchrotron scanning reveals amphibious ecomorphology in a new clade of bird-like dinosaurs. Nature, 552(7685): 395–399

Cau A, 2018. The assembly of the avian body plan: A 160-million-year long process. Bollettino della Società Paleontologica Italiana, 57(1): 1–25

Chatterjee S, Templin R J, 2007. Biplane wing planform and flight performance of the feathered dinosaur Microraptor gui. Proceedings of the National Academy of Sciences, 104(5): 1576–1580

Chen R, Wang M, Dong L et al., 2025. Earliest short-tailed bird from the Late Jurassic of China. Nature, 638(8050): 441–448

Chiappe L M, Walker C A, 2002. Skeletal morphology and systematics of the Cretaceous Enantiornithes (Ornithothoraces: Enantiornithes). In: Chiappe L M and Witmer L M eds. Mesozoic birds-above the deads of dinosaurs. Berkeley, CA: University of California Press: 240–267

Chuong C-M, Wu P, Zhang F C et al., 2003. Adaptation to the sky: Defining the feather with integument fossils from mesozoic China and experimental evidence from molecular laboratories. Journal of experimental Zoology (Mol Dev Evol), 298B: 42–56

Czerkas S A, Yuan C, 2002. An arboreal maniraptoran from northeast China. In: Czerkas S J eds. Feathered dinosaurs and the origin of flight Blanding: The Dinosaur Museum: 63–95

Dudley R, 1998. Atmospheric oxygen, giant Paleozoic insects and the evolution of aerial locomotor performance. Joural of Experimental Biology, 201: 1043–1050

Dyke G, De Kat R, Palmer C et al., 2013. Aerodynamic performance of the feathered dinosaur Microraptor and the evolution of feathered flight. Nature communications, 4: 2489

Evangelista D, Cardona G, Guenther-Gleason E et al., 2014. Aerodynamic characteristics of a feathered dinosaur measured using physical models. Effects of form on static stability and control effectiveness. Plos One, 9(1): e85203

Feduccia A, Tordoff H B, 1979. Feathers of Archaeopteryx: asymmetric vanes indicate aerodynamic function. Science, 203: 1021–1022

Feduccia A (1999). The origin and evolution of birds, 2nd ed. New Haven, Yale University Press.

Feo T J, Field D J, Prum R O, 2015. Barb geometry of asymmetrical feathers reveals a transitional morphology in the evolution of avian flight. Proceedings of the Royal Society B-Biological Sciences, 282(1803): 20142864

Forster C A, Sampson S D, Chiappe L M et al., 1998. The Theropod Ancestry of Birds: New Evidence from the Late Cretaceous of Madagascar. Science, 279(5358): 1915–1919

Forster C A, Chiappe L M, O'Connor P M et al., 2020. The osteology of the Late Cretaceous paravian Rahonavis ostromi from Madagascar. Palaeontol Electron, 23(2): a29

Foth C, Tischlinger H, Rauhut O W M, 2014. New specimen of Archaeopteryx provides insights into the evolution of pennaceous feathers. Nature, 511(7507): 79–82

Foth C, Rauhut O W M, 2017. Re-evaluation of the Haarlem Archaeopteryx and the radiation of maniraptoran theropod dinosaurs. BMC Evolutionary Biology, 17(1): 236

Foth C, Rauhut O (2020). The evolution of feathers-from their origin to the present. Switzerland, Springer.

Gianechini F A, Makovicky P J, Apesteguía S et al., 2018. Postcranial skeletal anatomy of the holotype and referred specimens of Buitreraptor gonzalezorum Makovicky, Apesteguía and Agnolín 2005 (Theropoda, Dromaeosauridae), from the Late Cretaceous of Patagonia. PeerJ, 6: e4558

Glen C L, Bennett M B, 2007. Foraging modes of Mesozoic birds and non-avian theropods. Current Biology, 17: R911–R912

Godefroit P, Demuynck H, Dyke G et al., 2013. Reduced plumage and flight ability of a new Jurassic paravian theropod from China. Nature communications, 4: 1394

Hartman S, Mortimer M, Wahl W R et al., 2019. A new paravian dinosaur from the Late Jurassic of North America supports a late acquisition of avian flight. PeerJ, 7: e7247

Hu D Y, Hou L-H, Zhang L J et al., 2009. A pre-Archaeopteryx troodontid from China with long feathers on the metatarsus. Nature, 461: 640–643

Hu D Y, Clarke J A, Eliason C M et al., 2018. A bony-crested Jurassic dinosaur with evidence of iridescent plumage highlights complexity in early paravian evolution. Nature communications, 9(1): 217

Hwang S H, Norell M A, Ji Q et al., 2002. New specimens of Microraptor zhaoianus (Theropoda: Dromaeosauridae) from northeastern China. American Museum Novitates, 3381: 1–44

Kellner A, Wang X L, Tischlinger H et al., 2010. The soft tissue of Jeholopterus (Pterosauria, Anurognathidae) and the structure of the pterosaur wing membrane. Proceedings of the Royal Society B-Biological Sciences, 277(1679): 321–330

Kiat Y, O'Connor J K, 2024. Functional constraints on the number and shape of flight feathers. Proceeding of the National Academy of Sciences of the United States of America, 121(8): e2306639121

Lee S, Lee Y-N, Currie P J et al., 2022. A non-avian dinosaur with a streamlined body exhibits potential adaptations for swimming. Communications Biology, 5(1): 1185

Lefèvre U, Cau A, Cincotta A et al., 2017. A new Jurassic theropod from China documents a transitional step in the macrostructure of feathers. Science of Nature, 104(9-10): 74

Longrich N R, Currie P, 2009. A Microraptorine (Dinosauria - Dromaeosauridae) from the Late Cretaceous of North America. Proceedings of the National Academy of Sciences of the United States of America, 106(13): 5002–5007

Longrich Nicholas R, Vinther J, Meng Q J et al., 2012. Primitive wing feather arrangement in Archaeopteryx lithographica and Anchiornis huxleyi. Current Biology, 22(23): 2262–2267

Lovegrove J, Upchurch P, Barrett P M, 2024. Untangling the tree or unravelling the consensus? Recent developments in the quest to resolve the roadscale relationships within Dinosauria. Journal of Systematic Palaeontology, 22(1): 2345333

Lu J C, Brusatte S L, 2015. A large, short-armed, winged dromaeosaurid (Dinosauria: Theropoda) from the Early Cretaceous of China and its implications for feather evolution. Scientific Reports, 5: 11775

Lü J C (2005). Oviraptorid Dinosaurs from Southern China. Beijing, Gelogical Publishing House.

Makovicky P J, Norell M A, Clark J M et al., 2003. Osteology and relationships of Byronosaurus jaffei (Theropda: Troodontidae). American Museum Novitates, 3402: 1–32

Makovicky P J, Norell M A, 2004. Troodontidae. In: Weishampel D B, Dodson P and Osmólska H eds. The Dinosauria 2nd. edn. Berkeley: University of California Press: 184–195

Makovicky P J, Apesteguía S, Agnolin F L, 2005. The earliest dromaeosaurid theropod from South America. Nature, 437(7061): 1007–1011

Makovicky P J, Turner A, Xu X, 2026. Paraves. In: Weishample D, Barrett P, Makovicky Pet al eds. Dinosauria (the third edition). Cambridge: Cambridge University Press

Manafzadeh A R, Padian K, 2018. ROM mapping of ligamentous constraints on avian hip mobility: implications for extinct ornithodirans. Proceedings of the Royal Society B: Biological Sciences, 285(1879): 20180727

Maryanska T, Halszka O, Wolsan M, 2002. Avialan status for Oviraptorosauria. Acta Palaeontologica Polonica, 47(1): 97–116

Napoli J, Fabbri M, Ruebenstahl A et al., 2025. Reorganization of the theropod wrist preceded the origin of avian flight. Nature, 644: 699–705

Norell M A, Xu X, 2005. Feathered dinosaurs. Annu. Rev. Earth Planet. Sci., 33: 277–299

Novas F E, Puerta P F, 1997. New evidence concerning avian origins from the Late Cretaceous of Patagonia. Nature, 387(6631): 390–392

Novas F E, Pol D, 2005. New evidence on deinonychosaurian dinosaurs from the Late Cretaceous of Patagonia. Nature, 433(7028): 858–861

Novas F E, Pol D, Canale J I et al., 2009. A bizarre Cretaceous theropod dinosaur from Patagonia and the evolution of Gondwanan dromaeosaurids. Proceedings of the Royal Society B, 276(1659): 1101–1107

Novas F E, Brisson Egli F, Agnolin F L et al., 2018. Postcranial osteology of a new specimen of Buitreraptor gonzalezorum (Theropoda, Unenlagiidae). Cretaceous Research, 83: 127–167

Nudds R L, Dyke G J, 2010. Narrow Primary Feather Rachises in Confuciusornis and Archaeopteryx Suggest Poor Flight Ability. Science, 328: 887–889

Osmólska H, Currie P J, Barsbold R, 2004. Oviraptorosauria. In: Weishampel D B, Dodson P and Osmólska H eds. The Dinosauria. Berkeley: University of California Press: 165–183

Ostrom J H, 1969. Osteology of Deinonychus antirrhopus, an unusual theropod from the Lower Cretaceous of Montana. Peabody Museum Natural History Bulletin, 30: 1–165

Padian K, 2003. Four-Winged Dinosaurs, Bird Precursors, or Neither? BioScience, 53: 450–452

Palmer C, 2014. The aerodynamics of gliding flight and its application to the arboreal flight of the Chinese feathered dinosaur Microraptor. Biological Journal of the Linnean Society, 113(3): 828–835

Pei R, Li Q G, Meng Q J et al., 2017. New specimens of Anchiornis huxleyi (Theropoda: Paraves) from the Late Jurassic of northeastern China. Bulletin of the American Museum of Natural History(411): 1–67

Pei R, Pittman M, Goloboff P A et al., 2020. Potential for powered flight neared by most close avialan relatives, but few crossed its thresholds. Current Biology, 30: 4033–4046

Pittman M, Xu X (2020). Pennaraptoran theropod dinosaurs: past progress and new frontiers. New York, American Museum of Natural History.

Rick J, Brock C, Lewanski A et al., 2024. Reference genome choice and filtering thresholds jointly influence phylogenomic analyses. Syst. Biol., 73(1): 76–101

Saitta E T, Rogers C, Brooker R A et al., 2017. Low fossilization potential of keratin protein revealed by experimental taphonomy. Palaeontology, 60: 547–556

Senter P, Barsbold R, Britt B B et al., 2004. Systematics and evolution of Dromaeosauridae (Dinosauria, theropoda). Bulletin of the Gunma Museum of Natural History, 8: 1–20

Senter P, 2006. Scapular orientation in theropods and basal birds and the origin of flapping flight. Acta Palaeontologica Polonica, 51(2): 305–313

Shen C Z, Zhao B, Gao C L et al., 2017. A new troodontid dinosaur (Liaoningvenator curriei gen. et sp. nov.) from the Early Cretaceous Yixian Formation in western Liaoning Province. Acta Geoscientica Sinica, 38(3): 359–371

Shipman P (1998). Take wing-Archaeopteryx and evolution of bird flight. London, The Guernsey Press Co. Ltd.

Soltis D E, Soltis P S, 1998. Choosing an approach and an appropriate gene for phylogenetic analysis. In: Soltis D E, Soltis P S and Doyle J J eds. Molecular Systematics of Plants II. Boston: Springer: 1–42

Turner A, H., Makovicky P J, Norell M A, 2012. A review of dromaeosaurid systematics and paravian phylogeny. Bulletin of the American Museum of Natural History, 371: 1–206

Voeten D F, Cubo J, Margerie E et al., 2018. Wing bone geometry reveals active flight in Archaeopteryx. Nature communications, 9(1): 923

Wang M, Wang X L, Zheng X T et al., 2025. Cranial anatomy of Anchiornis huxleyi (Theropoda: Paraves) sheds new light on bird skull evolution. Vertebrata PalAsiatica, 63(1): 20–42

Wellnhofer P (2009). Archaeopteryx-the icon of evolution. München, Verlag Dr. Friedrich Pfeil.

Xu L, Wang M, Zhou Z, 2023. A new avialan theropod from an emerging Jurassic terrestrial fauna. Nature, 621: 336–343

Xu X, Wang X L, Wu X C, 1999. A dromaeosaurid dinosaur with a filamentous integument from the Yixian Formation of China. Nature, 401(6750): 262–266

Xu X, Wang X L, 2000. Troodontid-like pes in the dromaeosaurid Sinornithosaurus. Paleontology Society of Korea, Special Publication, 2000(4): 179–188

Xu X, Zhou Z-H, Wang X-L, 2000. The smallest known non-avian theropod dinosaur. Nature, 408: 705–708

Xu X, Wu X C, 2001. Cranial morphology of Sinornithosaurus millenii Xu et al. 1999 (Dinosauria: Theropoda: Dromaeosauridae) from the Yixian Formation of Liaoning, China. Canadian Journal of Earth Sciences, 38(12): 1739–1752

Xu X (2002). Deinonychosaurian Fossils from the Jehol Group of Western Liaoning and the Coelurosaurian Evolution. Ph.D. Dissertation, Chinese Academy of Sciences.

Xu X, Zhang X H, Sereno P et al., 2002. A new therizinosauroid (Dinosauria,theropoda) from the upper Cretaceous Iren Dabasu Formation of Nei Mongol. Vertebrata PalAsiatica, 40(3): 228–240

Xu X, Wang X L, 2003. A new maniraptoran dinosaur from the Early Cretacous Yixian Formation of western Liaoning. Vertebrata PalAsiatica, 41(3): 195–202

Xu X, Zhou Z H, Wang X L et al., 2003. Four-winged dinosaurs from China. Nature, 421(6921): 335–340

Xu X, Wang X L, 2004. A new dromaeosaur (Dinosauria: Theropoda) from the Early Cretaceous Yixian Formation of western Liaoning. Vertebrata PalAsiatica, 42(2): 111–119

Xu X, Zhang F C, 2005. A new maniraptoran dinosaur from China with long feathers on the metatarsus. Naturwissenschaften, 92(4): 173–177

Xu X, Clark J M, Mo J-Y et al., 2009a. A Jurassic ceratosaur from China helps clarify avian digit homologies. Nature, 459: 940–944

Xu X, Zhao Q, Norell M et al., 2009b. A new feathered maniraptoran dinosaur fossil that fills a morphological gap in avian origin. Chinese Science Bulletin 54: 430–435

Xu X, You H, Du K et al., 2011. An Archaeopteryx-like theropod from China and the origin of Avialae. Nature, 475: 465–470

Xu X, 2012. Evolution: Taking wing with weak feathers. Current Biology, 22(23): R992–R994

Xu X, Sullivan C, Wang S, 2013. The systematic position of the enigmatic theropod dinosaur Yixianosaurus longimanus. Vertebrata PalAsiatica, 51(3): 169–183

Xu X, Han F L, Zhao Q, 2014a. Homologies and homeotic transformation of the theropod 'semilunate' carpal. Sci. Rep., 4: 6042

Xu X, Zhou Z H, Dudley R et al., 2014b. An integrative approach to understanding bird origins. Science, 346(6215): 1253293

Xu X, Zheng X T, Sullivan C et al., 2015. A bizarre Jurassic maniraptoran theropod with preserved evidence of membranous wings. Nature, 521(7550): 70–73

Xu X, Zhou Z H, Sullivan C et al., 2016. An updated review of the Middle-Late Jurassic Yanliao Biota: chronology, taphonomy, paleontology and paleoecology. Acta Geologica Sinica (English Edition), 90(6): 2229–2243

Xu X, 2024. Inferring aerial behavior in Mesozoic dinosaurs: implications and uncertainties. Proceeding of the National Academy of Sciences of the United States of America, 121(12): e2401482121

Xu X, Barrett P M, 2025. The origin and early evolution of feathers: implications, uncertainties and future prospects. Biology Letters, 21: 20240517

Yang Z, Jiang B, McNamara M E et al., 2019. Pterosaur integumentary structures with complex feather-like branching. Nature Ecology & Evolution, 3(1): 24–30

Yu Z, Wang M, Li Y, Deng, C. & He, H. , 2021. New geochronological constraints for the Lower Cretaceous Jiufotang Formation in Jianchang Basin, NE China, and their implications for the late Jehol Biota. Palaeogeography, Palaeoclimatology, Palaeoecology, 583: 110657

Zhang F C, Zhou Z H, Xu X et al., 2002. A juvenile coelurosaurian theropod from China indicates arboreal habits. Naturwissenschaften, 89(9): 394–398

Zhang F C, Zhou Z H, Xu X et al., 2008. A bizarre Jurassic maniraptoran from China with elongate ribbon-like feathers. Nature, 455(7216): 1105–1108

Zheng X, Xu X, You H et al., 2010. A short-armed dromaeosaurid from the Jehol Group of China with implications for early dromaeosaurid evolution. Proc. Biol. Sci., 277(1679): 211–217

Zheng X T, Zhou Z H, Wang X L et al., 2013. Hind Wings in Basal Birds and the Evolution of Leg Feathers. Science, 339(6125): 1309–1312

Zhou Z H, Zhang F C, 2002. A long-tailed, seed-eating bird from the Early Cretaceous of China. Nature, 418(6896): 405–409